UPPSALA UNIVERSITET

NATURGEOGRAFISKA

INSTITUTIONEN

AVDELNINGEN FÖR NATURGEOGRAFI

ROGER LeB HOOKE

SHEAR-STRESS AND SEDIMENT DISTRIBUTION IN A MEANDER BEND

UPPSALA 1974

UNGI RAPPORT 30

FÖRTECKNING ÖVER HITTILLS PUBLICERADE RAPPORTER

Nr 1 Sundborg, Å., 1969: The Need of Hydrological Training in Certain African Countries. An Account of a Tour in Africa between 25 April and 7 June 1969.

Nr 2 Nilsson, B., 1969: Development of a Depth-Integrating Water Sampler.

Nr 3 Kvarnäs, H. & Lindell, T., 1970: Hydrologiska studier i Ekoln. Rapport över hydrologisk verksamhet inom Naturvårdsverkets Limnologiska Undersökning januari-augusti 1969.

Nr 4 Nilsson, B., 1971: Sedimenttransport i svenska vattendrag. Ett IHD-projekt. Del 1. Metodik. Sediment Transport in Swedish Rivers. An IHD-Project. Part 1. Methods.

Nr 5 Bergqvist, E., 1971: Nåsten och Marsta - två mindre dräneringsområden vid Uppsala. Del 1. Målsättning och områdesbeskrivning. Nåsten and Marsta - Two Small Drainage Basins in Central Sweden. Part 1. Purpose of the Investigation and Description of the Basin.

Nr 6 Bergqvist, E., 1971: Nåsten och Marsta - två mindre dräneringsområden vid Uppsala. Del 2. Nederbörden. Nåsten and Marsta - Two Small Drainage Basins in Central Sweden. Part 2. Precipitation.

Nr 7 Bergqvist, E., 1971: Nåsten och Marsta - två mindre dräneringsområden vid Uppsala. Del 3. Snötaxeringar och snötäckets lokala variationer. Nåsten och Marsta - Two Small Drainage Basins in Central Sweden. Part 3. Snow Surveys and the Local Variations of the Snow Cover.

Nr 8 Bergqvist, E., 1971: Nåsten och Marsta - två mindre dräneringsområden vid Uppsala. Del 4. Avrinning samt transport av slam och lösta ämnen vid Stabby och Sundbro. Nåsten och Marsta - Two Small Drainage Basins in Central Sweden. Part 4. Runoff and Discharge of Suspended Matter and Dissolved Solids at Stabby and Sundbro.

Nr 9 Rutkis, J., 1971: Tables on Relative Relief in Middle and Western Europe.

Nr 10 Lindström, E., 1971: Submoräna sediment och isrörelser i nordvästra Ångermanland. Submorainic Sediments and Ice Movements in N.W. Ångermanland, Sweden.

Nr 11 Axelsson, V. & Håkanson, L., 1971: Sambandet mellan kvicksilverförekomst och sedimentologisk miljö i Ekoln. Del 1. Målsättning och analysmetodik. The Relation between Mercury Distribution and Sedimentological Environment in Lake Ekoln. Part 1. Purpose and Methods of Analysis.

Nr 12 Hjorth, S., 1971: Torne och Kalix älvar. Del 1. Allmän beskrivning. The Torne and Kalix Rivers. Part 1. General Description.

Nr 13 Dahlskog, S., Damberg, A., Hårdén, P.O. & Liljelund, L.E., 1972: The Kvikkjokk Delta - a Progress Report on a Multidisciplinary Research Project on a Boreal Mountain - Lake Delta.

Nr 14 Axelsson, V. & Håkanson, L., 1972: Sambandet mellan kvicksilverförekomst och sedimentologisk miljö i Ekoln. Del 2. Sedimentens egenskaper och kvicksilverinnehåll. The Relation between Mercury Distribution and Sedimentological Environment in Lake Ekoln. Part 2. Sedimentary Properties and Mercury Content.

UPPSALA UNIVERSITET
NATURGEOGRAFISKA INSTITUTIONEN
BOX 554
751 22 UPPSALA 1

UNIVERSITY OF UPPSALA
DEPARTMENT OF PHYSICAL GEOGRAPHY
BOX 554
S-751 22 UPPSALA 1, SWEDEN

ROGER LeB HOOKE

SHEAR-STRESS AND SEDIMENT DISTRIBUTION IN A MEANDER BEND

UPPSALA 1974

UNGI RAPPORT 30

CONTENTS

LIST OF FIGURES

PREFACE

This study was done in 1972-73 at the University of Uppsala, Sweden, while the author was on sabbatical leave from the University of Minnesota. Research facilities and office space were very generously provided by Professors Åke Sundborg and John Norrman. K. Lindé and B. Dahlin assisted with data collection. The able technical assistance of E. Zetterström and S. Karlsson was essential to success of the project. Thank also go to Kjerstin Andersson and Assar Lindberg for drafting and photography respectively, and to all my friends in Uppsala for making my stay there so enjoyable.

Financial support was provided by the National Research Council of Sweden and the National Science Foundation of the United States (Grant GA 29194).

Roger LeB. Hooke
Department of Geology and Geophysics
University of Minnesota
Minneapolis, Minnesota 55455 USA

1 ABSTRACT

A one-meter wide, meandering flume with movable sand bed was utilized in these experiments. Uniform flow was established at discharges of 20, 35, and 50 l/sec. Velocities near the bed, the distribution of sediment in transport, bed geometry, and strength of secondary flow were determined at each discharge. Bed shear stress was assumed to be proportional to the square of the velocity near the bed. Bed shear stresses were also measured with a Preston Tube in a uniform 35 l/sec flow over a dune-free stabilized bed. The stabilized bed was molded to the geometry produced by the same flow over sand.

The zone of maximum bed shear stress, τ, and maximum sediment discharge, q_s, is on the point bar in the upstream part of the bend. It crosses the channel centerline in the middle or downstream part of the bend, and follows the concave or down-valley bank to the next point bar downstream. With increasing discharge, secondary currents increase in strength. Consequently the zone of maximum τ and q_s remains closer to the inside bank across the point bar, and crosses the channel centerline somewhat lower in the bend. Secondary currents were also stronger in the 35 l/sec over the stabilized bed than in the same flow over sand, apparently because no dunes were present to break up secondary flow in the former. The zone of maximum τ was consequently closer to the inside bank in the stabilized-bed run.

It appears that bed geometry is adjusted to provide, at each point on the bed, precisely the shear stress necessary to transport the sediment load supplied. For example the gradual decrease in depth along the down-valley side of the channel from the deep in one bend to the point bar in the next results in a continual acceleration of the flow, and hence in shear stresses here which are higher than average for the channel.

For many combinations of discharge, sediment discharge, and sediment character, straight channels are unstable in nature, and the commonly observed meander geometry is stable. To understand why this meander geometry is stable, we consider how displacements from the stable geometry set up forces tending to restore that geometry. From work done to date, it is hypothesized that channel width, W, is determined by cohesiveness of bank materials. The radius of curvature of the bend, R, is then determined by the fact that separation occurs when $R/W \lesssim 2.5$. Measurements of bank shear stress in movable-bed channels with different meander geometries are needed next.

2 INTRODUCTION

Leopold and Wolman (1960, p. 788) concluded a review paper on river meanders with the statement, "A quantitative explanation of the meandering process will require balancing the erosive stress produced by tangential shear of the flowing water and the comparable resisting stress provided by the bank material." The suggestion was timely, and indeed laboratory measurements of the distribution of shear stress in open channel bends were already in progress. This early work (Ippen and Drinker, 1962; B. Yen, 1965) was done in channels with trapezoidal cross sections. It showed that in such channels the highest velocities and highest bed shear stresses occurred on the insides of bends in the position occupied by depositional point bars in natural streams.

The apparent inconsistancy - a depositional feature in the position of highest bed shear - prompted further investigation in laboratory channels with more natural bed geometry. C. Yen (1970), for example, covered the bed of B. Yen's (1965) trapezoidal channel with loose sand and allowed the flow to mold the bed into an equilibrium form with a point bar on the inside of the bend and deep on the outside. He then molded a concrete bed with this geometry. In this channel the zone of high velocity and high shear stress on the inside of the bend was still present, and shear stresses in this zone were 30 percent higher than in the trapezoidal channel. C. Yen (1970) concluded that bed geometry was determined by the secondary or helical flow in the bend rather than by shear stress.

The present study was undertaken with a somewhat different view in mind. It is well known that sediment movement increases with shear stress once a critical shear for initiation of motion is exceeded. We therefore hypothesize that at every point on the bed, bed geometry is adjusted to provide precisely the shear stress necessary to transport the sediment load supplied to that point. Suga (1967) apparently also had this concept in mind in his study of bed geometry in bends. A simple example, based in part on qualitative observations during the present study, will illustrate the hypothesis.

We start with a plane bed. Much of the sediment transported by the flow tends to move on the down-valley side of the straight reach between bends, and thus appears near the inside bank in the bend. We suppose that shear stresses on the inside of the bend are not sufficient to transport all of the sediment supplied, although the shear stress here may indeed be higher than average for the channel. Obviously deposition must occur. Not so obviously, the shear stress increases, as indicated by C. Yen's results cited above. Qualitatively it appears that the deposition decreases the water depth without causing a proportional decrease in the velocity. Therefore the velocity gradient increases, thus in-

creasing the shear stress. Simultaneously the sediment load supplied to this area of the bed may decrease if some of the sediment is deflected outward by the growing point bar. Eventually a balance or equilibrium is reached in which the shear stress over the point bar can move the sediment load supplied.

On the outside of the bend, conversely, shear stresses are initially low but little or no sediment is moved to this area of the bed from upstream. Because the shear stress can remove more sediment than is supplied, erosion occurs. As the outside of the bend becomes deeper, the shear stress decreases (C. Yen, 1970) and the lateral slope off the point bar increases, thus increasing the sediment supply to this area of the bed. In due course, equilibrium is reached.

This model is similar to Mackin's (1948) model of a graded river. Paraphrased, Mackin said that a river at grade (equilibrium) was one which, over a period of years, was delicately adjusted to carry the sediment load supplied with the available discharge. Mackin emphasized adjustment of slope; if the river cannot carry the sediment load supplied, deposition will occur, thus increasing slope (and hence velocity and shear stress) until the sediment load can be carried. Conversely, a decrease in slope occurs through degradation if the river can carry more sediment than is being supplied.

It is axiomatic that deposition will occur if more sediment is brought into an area than can be removed from it, and conversely. It follows that there is an equilibrium state in which the amount of sediment brought into an area equals that which can be removed from it. In many geomorphic systems, dependent variables are adjusted to provide this or some similar type of equilibrium. The equilibrium is usually stable, in that any small departure from it will set up forces tending to restore it. Through application of these principles, the relationship between process and land form may often be clarified. Mackin applied these principles to the problem of river slope. In the present paper we apply them to the problem of bed geomtry in a meander bend.

3 EXPERIMENTAL PROCEDURE

In the present experiments, the distribution of bed shear stress and the distribution of sediment in transport were measured at discharges of 20, 35, and 50 l/sec in a closed-circuit, recirculating, meandering flume (Fig. 1). Bed topography and the "strength" of secondary currents, or "helix strength", were determined at these discharges, and also at a discharge of 10 l/sec. Finally shear stress and "helix strength" measurements were made in a 35 l/sec flow over a concrete bed molded to the form of the bed developed by the same discharge over sand. Results of these measurements are presented in contour maps in Figs. 10 through 13. Details of the channel design and measurement techniques follow.

3.1 CHANNEL GEOMETRY

The centerline geometry of the flume was based on the sine-generated curve of Langbein and Leopold (1966),

$$\phi = \omega \operatorname{Sin} \frac{2 \pi m}{M} \tag{1}$$

because empirically this curve closely resembles the geometry of natural meanders, and because it provides a more gradual transition from straight reach to bend than do geometries consisting of a constant-radius circular arc and tangent to the arc. In this equation, ϕ is the angle which the channel centerline makes with respect to the down-valley direction at a point a distance m from the origin measured along the channel centerline, ω is the angle which the centerline makes with the valley axis at the origin (Fig. 1), and M is the length of the channel centerline over one meander wavelength. The geometry of the channel centerline, including the wavelength, λ, is thus completely specified by M and ω.

Channel width was determined from the well-known empirical relationship between width and wavelength,

$$\lambda = a W^b \tag{2}$$

where a ranges from 7 to 11 and $b \doteq 1$ (Leopold and Wolman, 1960).

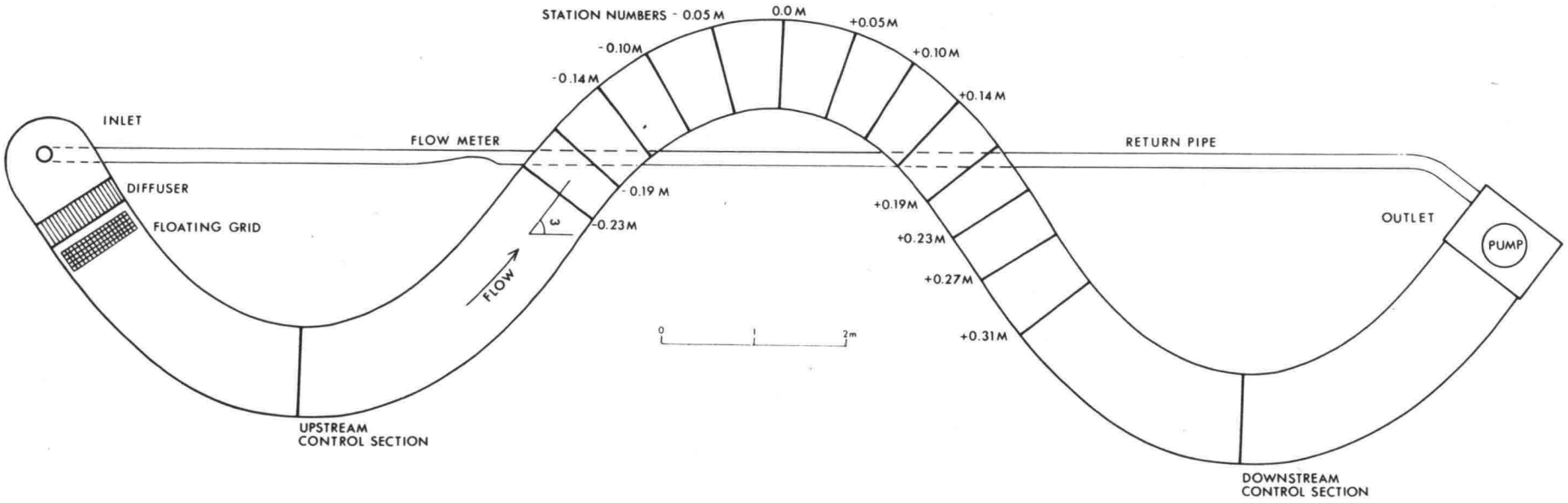

Fig. 1 Plan view of meandering channel.

Table 1 Summary of experimental data.

Run	Discharge, Q, l/sec	Mean depth, d, cm	Mean bed hydraulic radius r_b, cm	Mean velocity, cm/sec	Froude number	Mean slope of energy grade line	Bed friction factor $8\,gr_bS/V^2$	Width/depth ratio	Mean bed Shear stres $\tau = pgr_bS$ dynes/cm^2	Total sediment discharge Q_s, cm^3/sec
10	10	5.2	5.1	19.2	0.27	0.00213	0.23	19	11	0.19
20	20	7.3	7.1	27.5	0.33	0.00207	0.15	14	14	2.0
35	35	9.5	9.2	36.8	0.38	0.00221	0.12	11	20	8.0
35S	35	9.2	8.5	38.0	0.40	0.00101	0.047	11	8	0
50	50.5	12.8	12.2	39.4	0.35	0.00223	0.14	8	27	20.1

It was found that a channel with $\omega = 55^o$, M = 13.2 m, and W = 1.0 m would fit conveniently in the space available. With these values of M and ω, λ = 10.33 m. For comparison, the Yens' (1965, 1970) channel was designed with $\omega = 45^o$, λ = 30.2 m, and W = 2.34 m; Ippen and Drinker's (1962) flume had a single bend with $\omega = 30^o$; and the mean of 45 values of ω measured from Friedkin's (1945) maps of channels developed in non-cohesive sands was 57^o.

A number of factors were considered in selecting depth, velocity and slope for the various runs. First, it was desired to keep the width-depth ratio, W/d, within the range of values commonly observed in nature. Schumm (1960) measured width-depth ratios in nearly 50 channels and found values ranging from less than 3 to over 300. Width-depth ratios between 7 and 10 and between 20 and 50 were most common. To facilitate measurement in the laboratory channel, relatively large depths were desireable, so width-depth ratios between 8 and 20 were used (Table 1).

To make the model dynamically similar to natural meandering rivers, Froude similarly was used. Froude numbers of over 100 rivers at mean-annual discharge were calculated from data presented by Leopold and Maddock (1953). Values ranged from essentially zero to about 0.5. The median was 0.2. In the present experiment, Froude numbers ranged from 0.27 to 0.40 (Table 1).

The channel was constructed of cement blocks and lined with concrete. Walls were vertical at the top, and generally met the bed at right angles. However on the outsides of the three bends, a rounded corner with radius of about 10 cm was molded between bed and banks. The bed of the flume was covered with several centimeters of well-sorted sand with a geometric mean diameter of 0.30 mm (Fig. 2). At higher discharges the rounded corner of the concrete bed was exposed on the outsides of the bends, and the flat bed was occasionally exposed in troughs between dunes.

During initial tests it was found that to obtain the desired range of width-depth ratios and Froude numbers in flows over this sand, an energy-gradeline slope of about 0.002 was required. It was therefore decided to run all experiments at approximately this slope, thus simulating a natural river with seasonal changes in discharge at a-station.

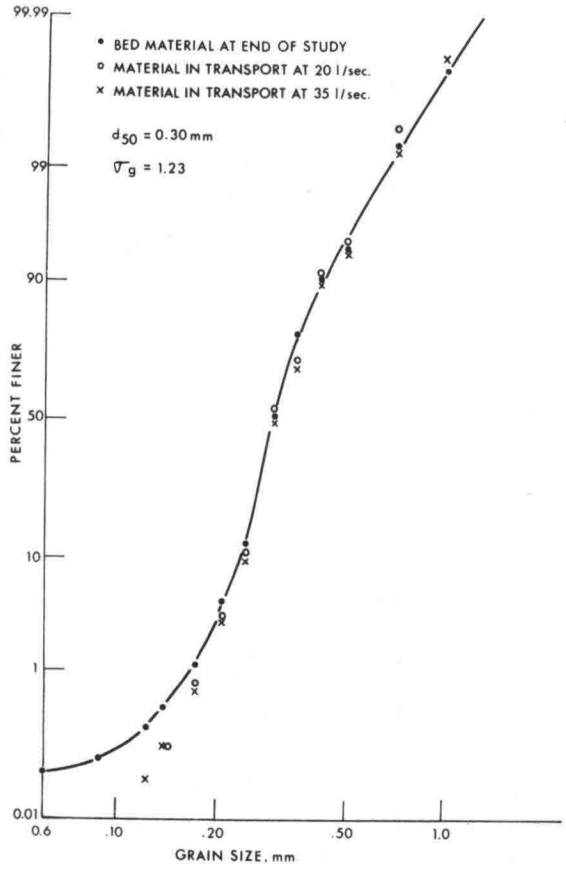

Fig. 2 Grain-size analyses of sand used.

3.2 DISCHARGE, DEPTH, AND SLOPE MEASUREMENTS

Discharge was controlled by varying pump speed and was measured with the use of a "top contraction meter" in the 15-cm diameter return line (Fig. 1). The meter was calibrated[1] by discharging water through it into a basin above a V-notch weir which had been calibrated previously. Water flowed over the weir into the flume inlet, thus completing the closed system. All sand was removed from the flume during calibration.

In the test reach (middle bend of Fig. 1), water-surface and bed elevation measurements were made with the use of a point gage mounted on a carriage which traveled on rails paralleling the sides of the flume. At the upstream and downstream control sections similar measurements were made with a point gage which moved on a rail crossing the channel.

Initially (Run 20)[2] water-surface slope was determined by measuring water-

---

[1] The discharge coefficient obtained (Rouse, 1950, p. 204, eqn. 4) was 0.9285 for flows above 25 l/sec. At lower discharges a slightly lower coefficient should be used. A value of 0.91 is appropriate at 17 l/sec. The final calibration equation was $Q = 6.654\sqrt{h}$ where h is in cm of water head and Q is in l/sec.

[2] For convenience, runs are assigned numbers numerically equal to the discharge in liters/second. This does not imply that 20 runs were made, nor that this was the 20th run in the series. In fact it was the first complete run.

surface elevations at the two control sections. Later, static tubes were placed in identical locations in each of the three bends. These tubes were connected to pots mounted next to the rail at Station 0.0M (Fig. 1), and water elevations in the pots were read with the use of a point gage which rode on the rail. A pressure transducer was placed between the pots connected to static tubes in the two control sections, and the head difference between these two pots was recorded continuously during all runs except Run 20. Random variations in water surface elevation in the pots could thus be recognized, and the mean water surface slope estimated.

Slope increased with time due to loss of water from the system through evaporation. This loss averaged about 2 mm per day, thus resulting in a decrease in depth of about 2%, and a consequent increase in water surface slope of about 6%. Because runs commonly lasted 15 to 20 days, it was important to determine such losses and correct for them daily. This could be done best by stopping the flow and measuring the elevation of the quiet water surface. However stopping and restarting the flow caused undesireable disturbance of the bed, so this was done frequently only at higher discharges where higher sediment transport rates quickly eliminated these disturbances.At lower discharges, the amount of water to be added was estimated from the relation $(d_i/d_f)^3 = S_f/S_i$ where $\underline{S}$ and $\underline{d}$ are slope and depth respectively, and the subscripts $\underline{i}$ and $\underline{f}$ refer to the situation before water was added and after respectively. $S_f = 0.002$.

At the end of a run, water surface elevations were measured at three points at each of the 14 stations and two control sections (Fig. 1). The flow was then stopped and local bed forms were smoothed before measuring bed elevations. In smoothing, the object was to displace sand from dune crests into adjacent troughs. Thus bed elevations measured were averages over an area roughly two dune wavelengths in diameter. Mean water depths at each section were calculated, as was the total head, $H = h_{ws} + V^2/2g$, where h_{ws} is the mean elevation of the water surface above some arbitrary datum, and V is the mean velocity in the section. The mean slope of the energy grade line (Table 1) was determined by a least - squares procedure. This is considered to be a reasonable estimate of the mean slope during a run.

Energy grade lines are plotted in Fig. 3. Lines drawn through the points were adjusted so that water surface slopes were equal at points M/2 apart, as required by symmetry. As expected (e.g. Ippen and Drinker, 1962; B. Yen, 1965, p. 63), the energy loss is higher in the bends than in the straight reaches. This effect is more pronounced at higher discharges (depths), as observed by Onishi et.al. (1972).

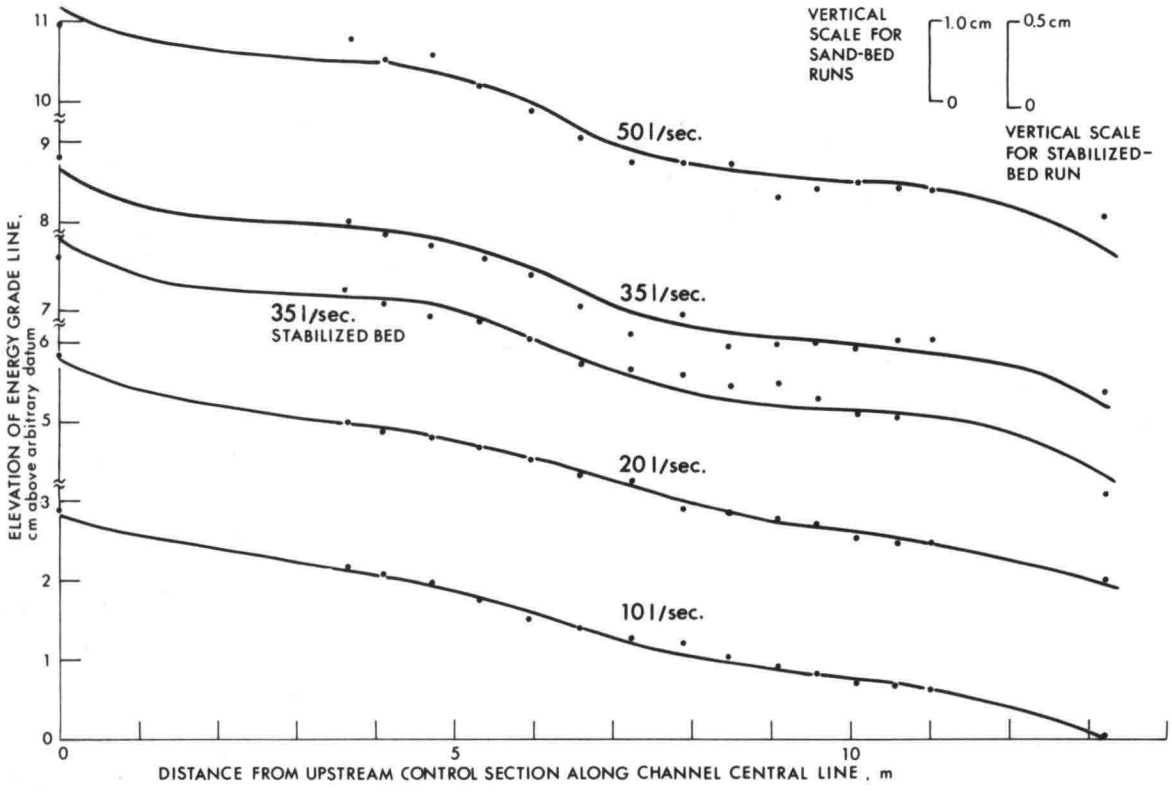

Fig. 3 Energy grade lines for various discharge. Datum varies between runs. Vertical scale for Run 35S (stabilized bed) is .00221/.00101 = 2.2 times that for other runs to facilitate comparison with Run 35.

3.3 EQUILIBRIUM

Equilibrium was assumed to exist when: (1) the mean water-surface slope between the two control sections remained close to 0.002 for a number of hours; (2) the difference between the mean water-surface slope in the upstream half of the flume (between the upstream control section and station 0.0M (Fig. 1)) and that in the downstream half was less than about 10% of the mean; and, (3) gross bed geometry did not change through time. In Run 20 the flow was run for approximately 150 hours before beginning measurements. In subsequent runs the initial running time was only about 50 hours. This was thought to be sufficient because slope was not changed between runs, and no major longitudinal redistribution of bed material was necessary.

It is not easy to demonstrate that a given flow in a movable-bed flume is uniform because local depth fluctuates with time due to movement of bed forms. Furthermore, in a meandering flume, depth is a function of position, m, in the bend, so only measurements which are taken a distance M/2 apart can be compared. In the present experiments there were five such pairs of depth measurements. From these a uniformity index, $\overline{\Delta d}$, was calculated as follows:

$$\overline{\Delta d} = \frac{1}{n} \sum (d_m - d_{m+M/2})$$

where d_m is the mean depth a distance m from the upstream control section, and $d_{m+M/2}$ was the mean depth one half wavelength further downstream. The results are given in Table 2. Minus values indicate that depths tended to increase

downstream ($d_{m+M/2} > d_m$) and conversely. In the high discharge movable bed runs $\overline{\Delta d}$ is large enough to raise some question about the uniformity of the flow. However the number of observations, n, is small and during these two runs sand waves, with amplitudes of 6 to 10 cm and wavelengths of up to a meter moved along the down-valley banks in the straight reaches. Thus substantial transient variations in $\overline{\Delta d}$ are likely.

3.4 SEDIMENT DISCHARGE MEASUREMENTS

During Run 10, the total sediment discharge, Q_s, was determined by placing a trough across the outlet of the flume. This trough caught virtually all sediment in motion. Sediment was removed from the trough by siphoning and was returned to the system after measuring. Measurements were made four times during the run.

During runs at higher discharge the trap did not catch all of the sediment in motion. Therefore it was removed, and Q_s was measured at the point where the return pipe discharged vertically upward into the inlet. A 5 mm diameter sampling tube was used, and 25 one-liter samples were taken from an array of sampling points. Each sampling point subtended an area of 7.06 cm^2 in the pipe mouth. Velocity in the sampling tube was adjusted to equal velocity in the pipe at the appropriate distance from the pipe wall. Two complete sets of samples were taken during each run, and the sediment discharge was calculated separately for each set (Fig. 4). The mean sediment discharge per unit width, q_s, was calculated by assuming a grain density of 2.7 g/cm^3 and 35% void space.

A primary objective of this study was to determine the planimetric distribution of q_s (Fig. 12). Two methods of measuring q_s were used. The first involved measurement of migration rates of ripples and dunes (Simons et.al., 1965). A circular, flat-bottomed, clear plastic dish, 10 cm in diameter and 2.3 cm high, was fastened to the instrument carriage and lowered until it touched the water surface. A scale graduated in millimeters was scribed on the bottom of the dish. A similar scale graduated in centimeters was scribed on a plastic plate and laid on top of the dish. A dune was selected for measurement and the instrument carriage and dish were positioned over the dune so that one of the lines scribed on the top plate was in line with one on the bottom of the dish and with the dune crest. The velocity of the dune crest was determined by timing it with a stop watch as it passed beneath the lower scale. The upper scale was used to preserve proper alignment of the eye with the lower scale and the dune crest. The length, δ,

Table 2 Flow uniformity.

Run	10	20	35	35S	50
Δd, cm	-0.03	-0.06	+0.8	+0.03	-1.1
$100\ \Delta d/\bar{d}$, %	-0.6	-0.8	+8.4	+0.3	-8.6

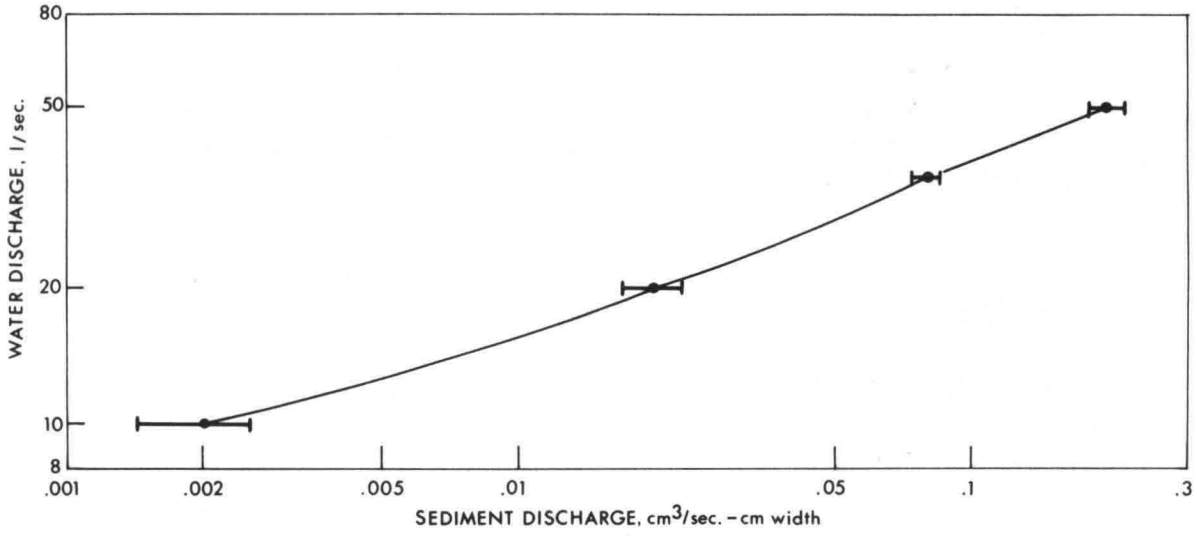

Fig. 4 Mean sediment discharge per unit width, q_s. Error bars show range of measured rates (see text).

of the horizontal projection of the dune slip face parallel to the channel centerline was measured with the lower scale at both the beginning and the end of the timing period. The angle, θ, that the dune crest made with a perpendicular to the channel centerline was also measured with a protractor scale on the upper plate. q_s was then calculated from:

$$q_s = \frac{1}{2} \frac{D + \frac{\delta_2 - \delta_1}{2}}{t} \quad \frac{\delta_1 + \delta_2}{2} \text{ Tan } a \text{ Cos}^3\theta \qquad (3)$$

where a is the angle of repose of the dune slip face, here taken to be 38°, and D is the distance moved in time t. To D is added one-half the change in length of the dune slip face, $(\delta_2 - \delta_1)/2$, where the subscripts 1 and 2 refer to the initial and final measurements of δ respectively. The distance moved, D, and mean length of slip face, $\frac{\delta_1 + \delta_2}{2}$ are miltiplied by Cos θ to obtain the sediment discharge perpendicular to the dune crest. The result is multiplied by Cos θ a third time to obtain the sediment discharge parallel to the channel center line. The result is divided by 2 because the transport rate is zero in dune troughs and rises to a maximum at the dune crest where it is measured (Simons et.al., 1965).

Dune migration rates were not noticeably affected by having the plastic dish in contact with the water surface. Even at shallow depths, any error due to the presence of the dish appeared to be small compared with normal stochastic variations in transport rate.

At discharges of 35 and 50 l/sec an appreciable fraction of the sediment moving over a dune crest was not trapped on the slip face, but instead continued on to the next dune downstream. Much of this material was not actually in suspension;

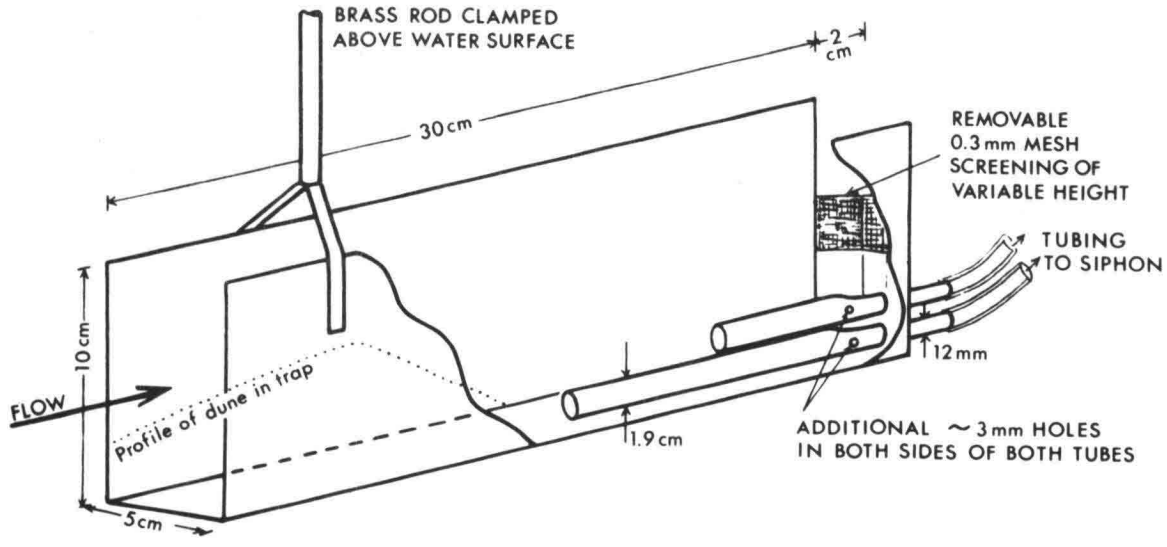

Fig. 5 Sediment trap for measuring q_s at higher velocities. Trap constructed of galvinized sheet metal with brass tubing.

rather it was swept laterally off the slip face and carried away by water passing around the sides of the dunes. Thus dune-migration measurements systematically underestimated q_s, and a sediment trap had to be used.

The trap, shown in Fig. 5, was pressed down into the bed so that the upstream bottom edge was always buried. Dunes migrated into the trap as shown, and material slumping down the slip face was removed by the siphons. With proper alignment, disturbances at the trap entrance were minimized. The part of a dune crest inside the trap remained in line with that outside until the former reached the first siphon. The removable screen at the back of the trap permitted some flexibility when working in relatively shallow areas, but in general was not really necessary. Similarly the 3 mm diameter holes near the downstream ends of the siphons were probably unnecessary, as sand rarely got this far back in the traps. Between 90 and 100 percent of the sand was removed by the lower siphon.

Visually it appeared that a small amount of suspended sediment might be passing through the trap over the screening. Therefore a third siphon with a rectangular opening 2 mm wide and 20 mm high was inserted immediately above the screen during a few tests. It was found that more than 97% of the material was being caught by the two primary siphons. Therefore use of this suspended load sampler was discontinued.

The discharge from the lower siphon was fed into a 1-liter graduate in which most of the sand was trapped. Water overflowed from the graduate into a bucket and then into a tank, whence it was pumped back into the flume. Sand which did not settle out in the graduate was trapped in the bucket. When a graduate contained between 500 and 1000 cm^3 of sand, it was replaced. The full graduate was tapped until no further settling of the sand occurred. Then sand volume and sampling time were recorded, and a short-term sediment discharge rate was calculated. These short-term rates are shown by horizontal lines on the vertical bars representing trap measurements in Figures 6B and 6C. Flow from the upper siphon was simply

fed into the bucket. At the end of a test, sand in the bucket was added to that collected by the graduates and the mean sediment discharge was calculated.

In a few tests the discharge from both siphons was fed into a bucket during most or all of the sampling period, so fewer short-term sediment-discharge rates were obtained. These are referred to as bucket samples.

Initially a sampling time of 45 to 60 minutes was used for each trap measurement. However transport rates proved to be remarkably variable (Fig. 6), so the standard sampling time was increased to 2 hours. Generally two traps were operated simultaneously at the same station.

At each station somewhere between 25 and 60 dune migration measurements and, at the higher discharges, 2 to 8 trap measurements were made (Figs. 6). Using these measurements as a guide, a line was drawn such that $\int q_s dx = Q_s$ as required by continuity. In Run 20 (Fig. 6A) the lower parts of these curves are fairly well defined by the dune migration measurements (see station 0.19M for example). It is more difficult to draw a reasonable line through the higher points, but with the area under the line specified, the curve here is also fairly closely controlled. The greatest uncertainty arises close to the wall on the high transport-rate side of the channel, as it is difficult to determine how abruptly the rate decreases to zero. Comparable uncertainty arises at some stations in the bend (e.g. Station 0.0M, Fig. 6A) where the low transport-rate side of the curve is no longer low enough to be well defined by the dune migration measurements.

In the higher discharge runs, the lower parts of some curves are reasonably defined by dune migration measurements (e.g. Sta-0.23M, Fig. 6B), but this is by no means always true (viz. Sta-0.19M, Fig. 6C). Furthermore, it is clear that the upper parts of these curves are inadequately controlled (e.g. Sta 0.0M, Fig. 6C). With a few trap measurements, however, a reasonable curve usually can be drawn (e.g. Sta 0.0M, Fig. 6C).

The curves in Figs. 6B and 6C were drawn according to the following rules:

a/ Dune migration rates were used to define the lower parts of the curves in the absence of trap measurements.

b/ The curve was initially drawn through the mean values of the trap measurements.

c/ Where the curved base of the channel wall was exposed (see p. 9 above), q_s was assumed to be zero (e.g. near outside bank between stations +0.05M and +0.14M in both Figs. 6B and 6C).

d/ The curves were assumed to be smooth and continuous, and to have only one maximum unless there was compelling evidence to the contrary (e.g. Sta 0.0M, Figs. 6B and 6C).

e/ Where the sediment-discharge continuity condition $\int q_s d_x = Q_s$, was not satisfied, the mean transport rate from each trap measurement was multiplied by a constant factor, thus increasing or decreasing the height of the curves by a constant percentage of the mean (viz. Sta +0.27M, Fig. 6C).

f/ Finally, extenuating factors were considered. For example on the right side of Sta-0.05M, Fig. 6B, it was felt that the trap measurement might be high because sand appeared to be slumping down the slope of the point bar into the trap mouth.

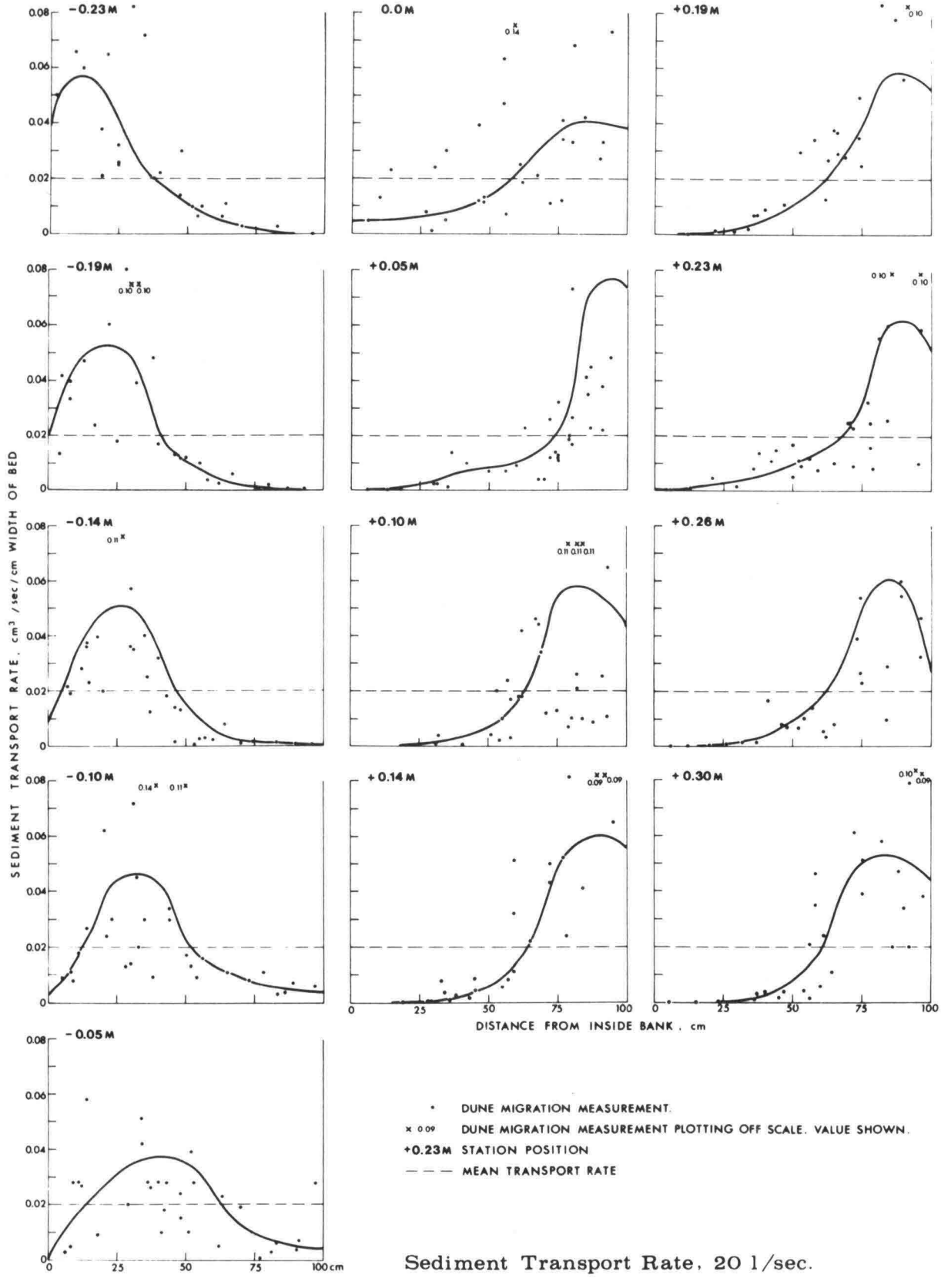

Fig. 6 Sediment discharge per unit width, q_s, at the various stations. Curves adjusted to make $\int q_s dx = Q_s$. Fig. 6A Run 20.

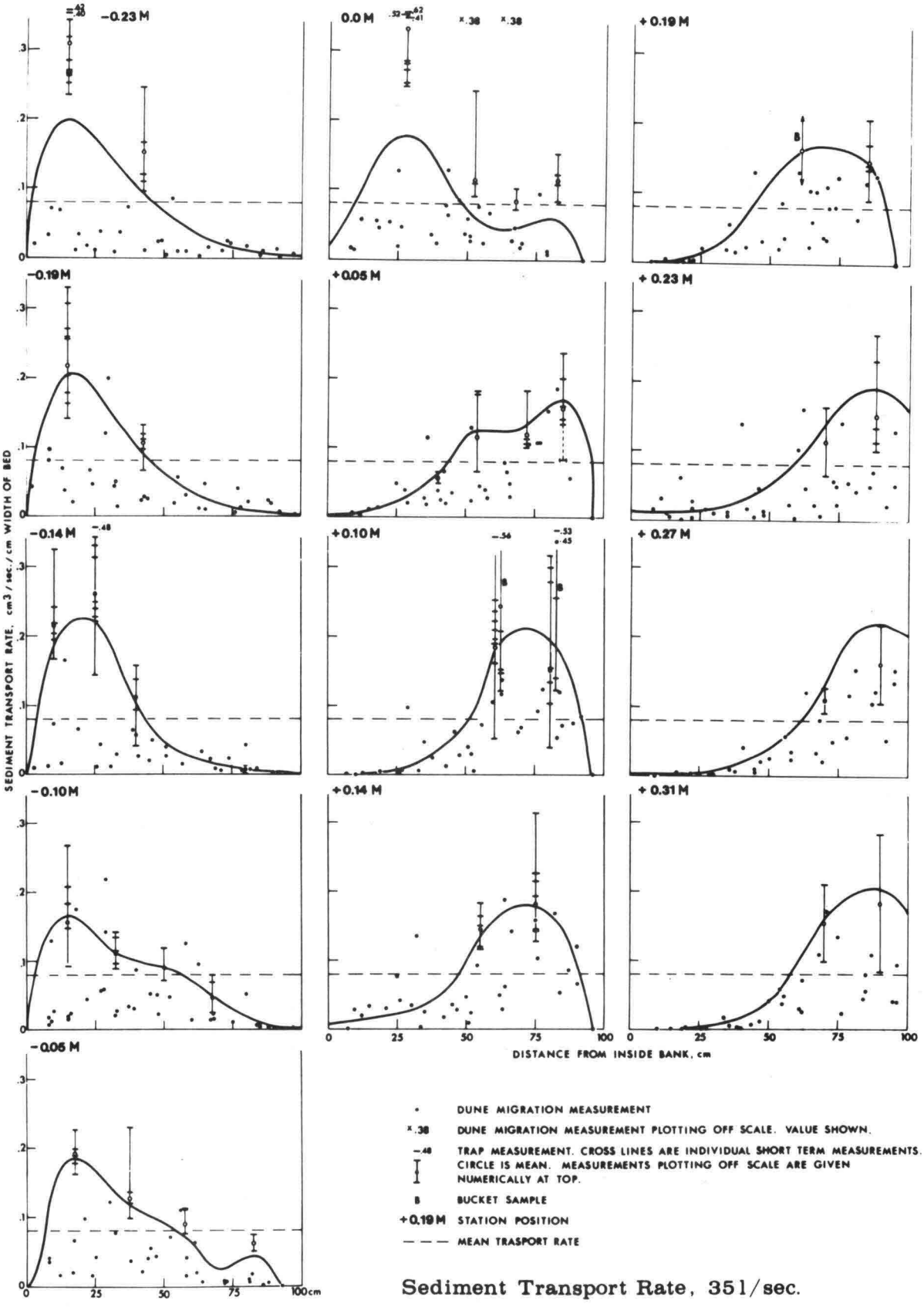

Sediment Transport Rate, 35 l/sec.

Fig. 6B Run 35.

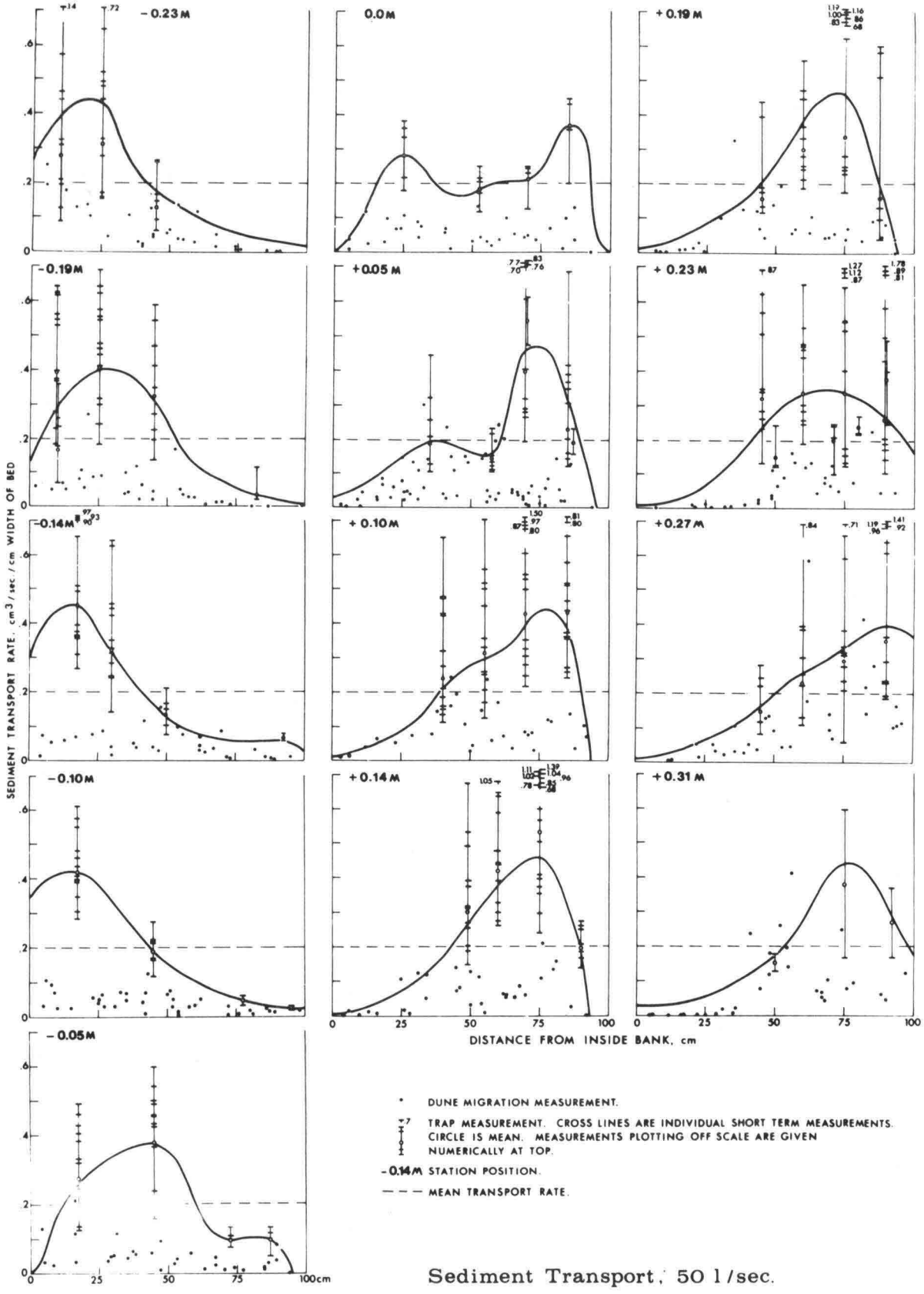
-0.23 M
0.0 M
+0.19 M
-0.19 M
+0.05 M
+0.23 M
-0.14 M
+0.10 M
+0.27 M
-0.10 M
+0.14 M
+0.31 M
-0.05 M
SEDIMENT TRANSPORT RATE, cm³/sec/cm WIDTH OF BED
DISTANCE FROM INSIDE BANK, cm
0
25
50
75
100
100cm
.2
.4
.6
DUNE MIGRATION MEASUREMENT.
TRAP MEASUREMENT. CROSS LINES ARE INDIVIDUAL SHORT TERM MEASUREMENTS. CIRCLE IS MEAN. MEASUREMENTS PLOTTING OFF SCALE ARE GIVEN NUMERICALLY AT TOP.
-0.14 M STATION POSITION.
MEAN TRANSPORT RATE.
Sediment Transport, 50 l/sec.

Fig. 6C Run 50.

In general curves for Run 50 (Fig. 6C) could be drawn close to the means of the trap measurements without violating the sediment-discharge continuity condition. This was not true for Run 35 (viz. Sta 0.0M, Fig. 6B), apparently because this run was in the transitional flow regime. The transitional regime is one in which the combination of discharge, mean depth, and bed-material size imposed on the system does not lead to a unique stable flow condition (Vanoni and Brooks, 1957). Different flow conditions exist simultaneously in different parts of the channel.

Discharge and bed-material size cannot vary with (longitudinal) position in the flume but depth can. Consequently if a particular combination of these independent variables is unstable, a sand wave forms. Over the sand wave the depth is lower than average for the flume, and the velocity and sediment discharge are higher. Thus the sand wave migrates continuously through the system. In straight flumes the bed is flat over the sand wave and dune-covered elsewhere (Brooks, 1958). Thus the sand wave is clearly defined, and its progress through the flume can be followed visually. In a meandering channel, however, secondary currents prevent development of the flat-bed regime. Consequently sand waves are more difficult to identify; the existence of the present one was suggested by the variability in sediment discharge rates obtained from trap measurements. Subsequently its front was identified entering the upstream end of the test section (Sta-0.23M). The average depth just downstream from the front (Sta's -0.19M and -0.14M) was 11.05 cm, while at the comparable positions one-half wavelength downstream it was 9.45 cm. The wave may have been quite long.

Ideally one would like to consider only those measurements made on top of the wave, or conversely. However no consistent interpretation of the data is possible from this point of view because, although most trap measurements fall close to curves in Fig. 6B, there are some that fall well above (Stations -0.23M, 0.0M, and +0.10M) and others well below (Stations +0.23M and +0.27M). Thus the curves shown in Fig. 6B, the shear-stress curves which follow, and the data listed in Table 1 for Run 35, are averages obtained from measurements on two flows with slightly different regimes. A flow regime with these characteristics does not, in fact, exist as a stable regime in this flume.

3.5 MOVABLE-BED SHEAR STRESS MEASUREMENTS

Bed shear stress is a very elusive quantity to measure. Most recent studies have employed the Preston Tube (Ippen and Drinker, 1962; B. Yen, 1965; C. Yen, 1970), but have failed to consider the fact that the von Kármán "constant", K, may not be constant in the presence of appreciable suspended sediment (Vanoni and Nomicos, 1959) or in curved channels (Rozovskii, 1957, p. 113-4 and 176-187). The von Kármán constant enters into the relationship between the pressure difference measured by the Preston Tube, ΔP, and the shear stress, τ, as follows:

$$\frac{\Delta P}{\tau} = \frac{C}{K^2} \quad . \tag{4}$$

C depends on tube geometry, on boundary roughness, and, in hydraulically smooth or transitional flow regimes, on boundary Reynolds number (Creager et.al., 1969; Hwang and Laursen, 1963). The boundary Reynolds number is $\frac{U_* k_s}{\nu}$ where U_* is the shear velocity, $\sqrt{\frac{\tau_o}{\rho}}$, k_s is the equivalent sand grain roughness, and ν is the kinematic viscosity. Because K is squared in equation (4), variations in K are important to consider. We will return to this problem in Section 5.

For the movable bed studies a 2 mm O.D. Preston Tube was positioned over a dune crest. The tube was viewed through a plastic dish set in contact with the water surface, and was lowered to the point where further lowering would have produced scour of the dune. It was maintained in this position, about 2 mm above the crest, by moving the instrument carriage with the advancing dune. The pressure difference, ΔP, was determined with the use of a water manometer inclined at 10^o. The reading on the manometer at $\Delta P = 0$ was checked frequently during the measurements.

In essence, the quantity measured was the velocity, U_{dc}, just above the dune crest. It was then assumed that the shear stress was proportional to this velocity squared, as indeed it is if the logarithmic velocity law holds, the von Kármán constant is constant, and all measurements are made the same distance above the bed.

Between 25 and 75 measurements were made at each station, and plotted as shown in Figs.7. Lines were drawn through the points and initially adjusted to make $\int \tau dx = \text{Const.}$ Then relative shear stress values were read from the curves at 10 evenly spaced points in each cross section. Sediment discharge rates, q_s, were obtained at the same points from the curves in Fig. 6. Shear stress was then plotted against sediment transport rate, as shown in Fig. 8, and a curve of the form

$$q_s = a\,(\tau - \tau_c)^b$$

was fitted to the points by eye. τ_c is the critical shear stress for initiation of motion. Finally the curves through the points in Figs. 7 were readjusted to satisfy the sediment-discharge continuity condition, now expressed as

$$\int a\,(\tau - \tau_c)^b\,dx = Q_s \qquad (5)$$

The curves shown in Figs. 7 satisfy this condition. Different values of the constants a and b were used for each run, but τ_c was assumed to be constant between runs. Replotting of the τ vs. q_s curves using the new τ values indicated that no further adjustment of the values of a and b was necessary.

Initially all calculations were carried out with the use of relative shear stress values. However in order to compare the equations relating q_s and τ for the various runs, it was necessary to convert the τ scale to dynes/cm^2 (Fig. 8). This was done with the use of the relation

$$\tau = \beta\, U_{dc}^2 \qquad (6)$$

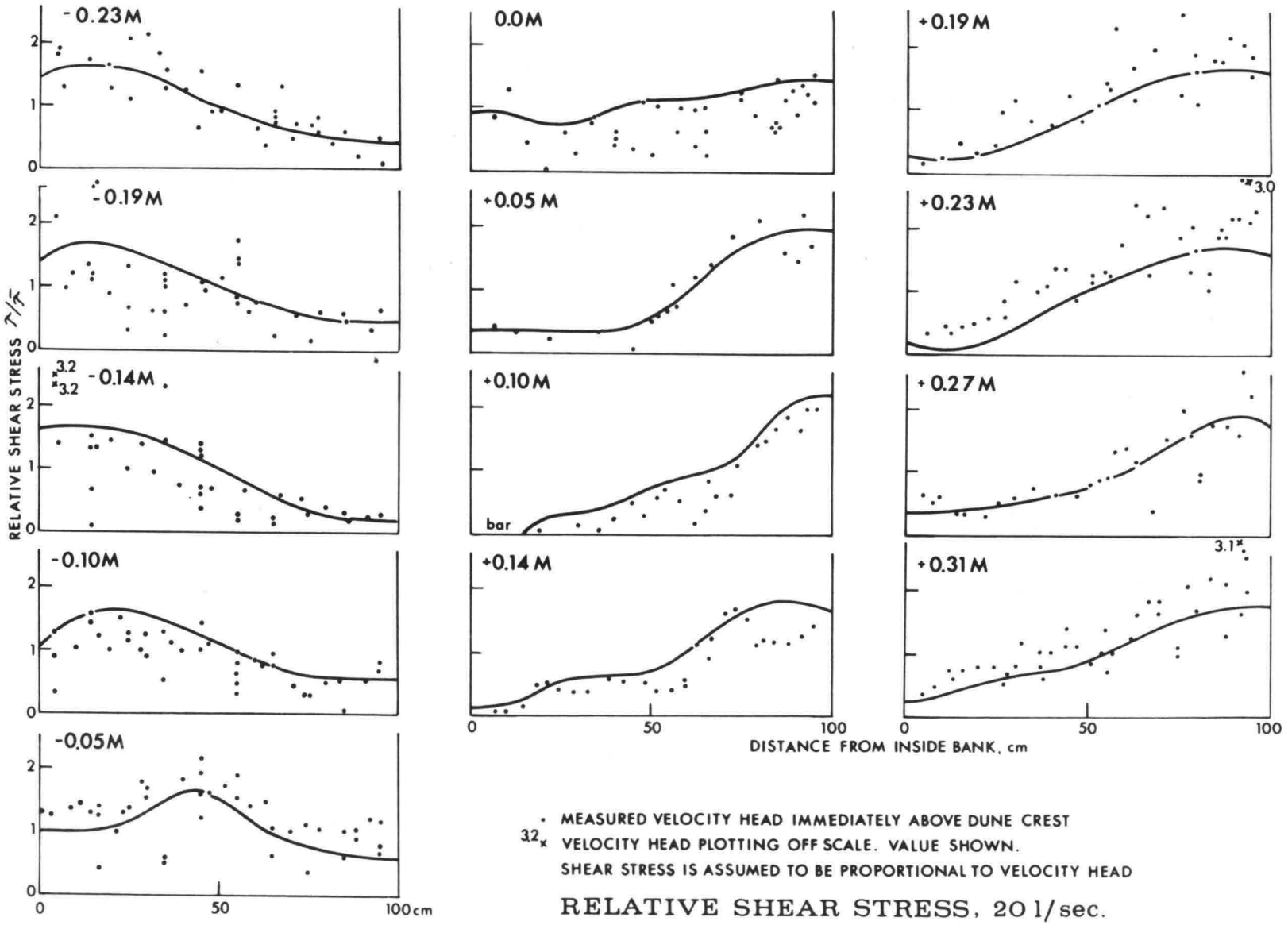

Fig. 7 Relative shear stress, $\tau/\bar{\tau}$, at the various stations. Curves adjusted to make $\int a(\tau - \tau_c)^b dx = Q_s$. Fig. 7A Run 20.

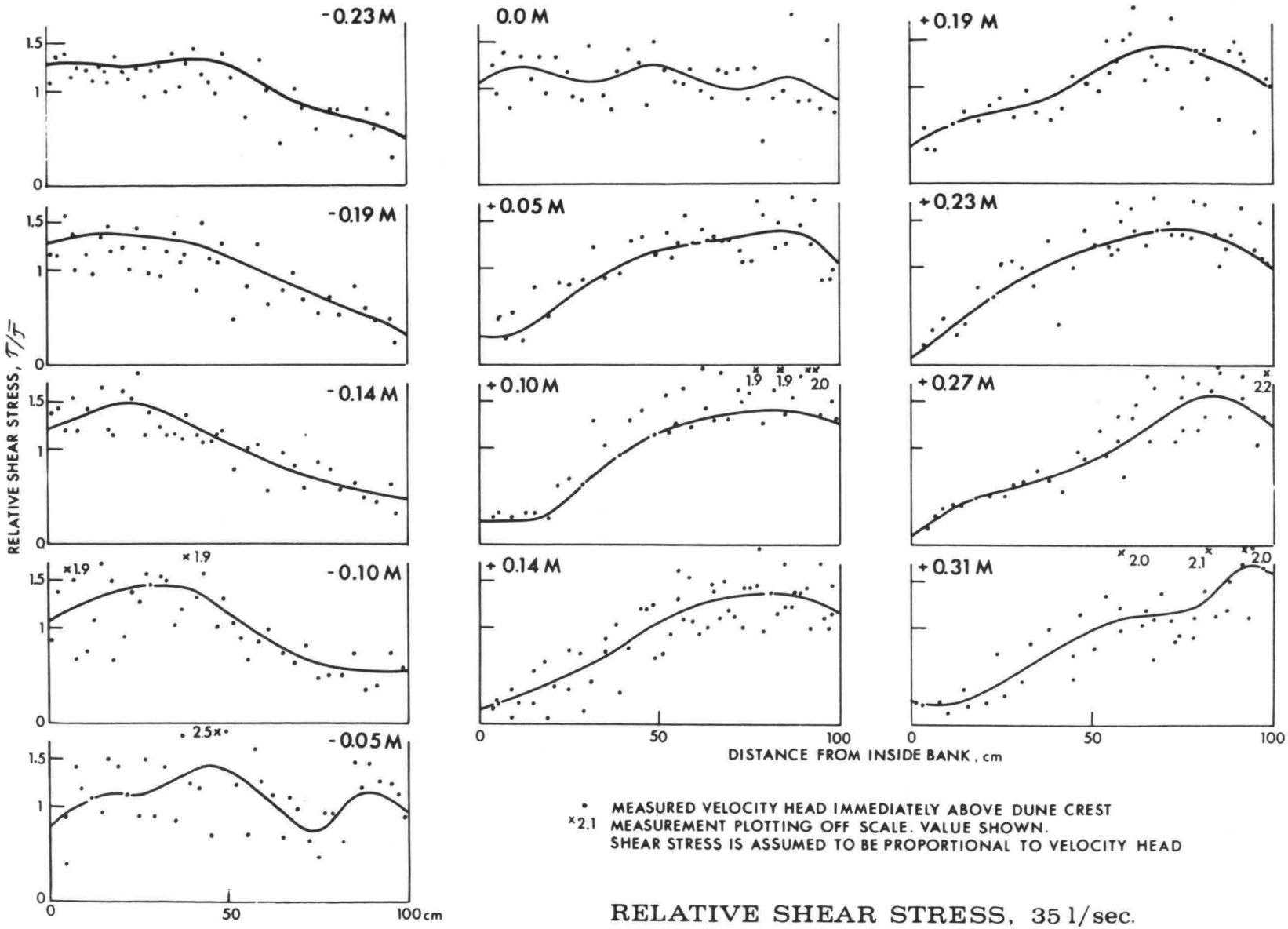
-0.23 M
0.0 M
+0.19 M
-0.19 M
+0.05 M
+0.23 M
-0.14 M
+0.10 M
+0.27 M
-0.10 M
+0.14 M
+0.31 M
-0.05 M
RELATIVE SHEAR STRESS, τ/τ̄
DISTANCE FROM INSIDE BANK, cm
0
50
100
100 cm
1.5
1
0
MEASURED VELOCITY HEAD IMMEDIATELY ABOVE DUNE CREST
×2.1 MEASUREMENT PLOTTING OFF SCALE. VALUE SHOWN.
SHEAR STRESS IS ASSUMED TO BE PROPORTIONAL TO VELOCITY HEAD
RELATIVE SHEAR STRESS, 35 l/sec.

Fig. 7B Run 35.

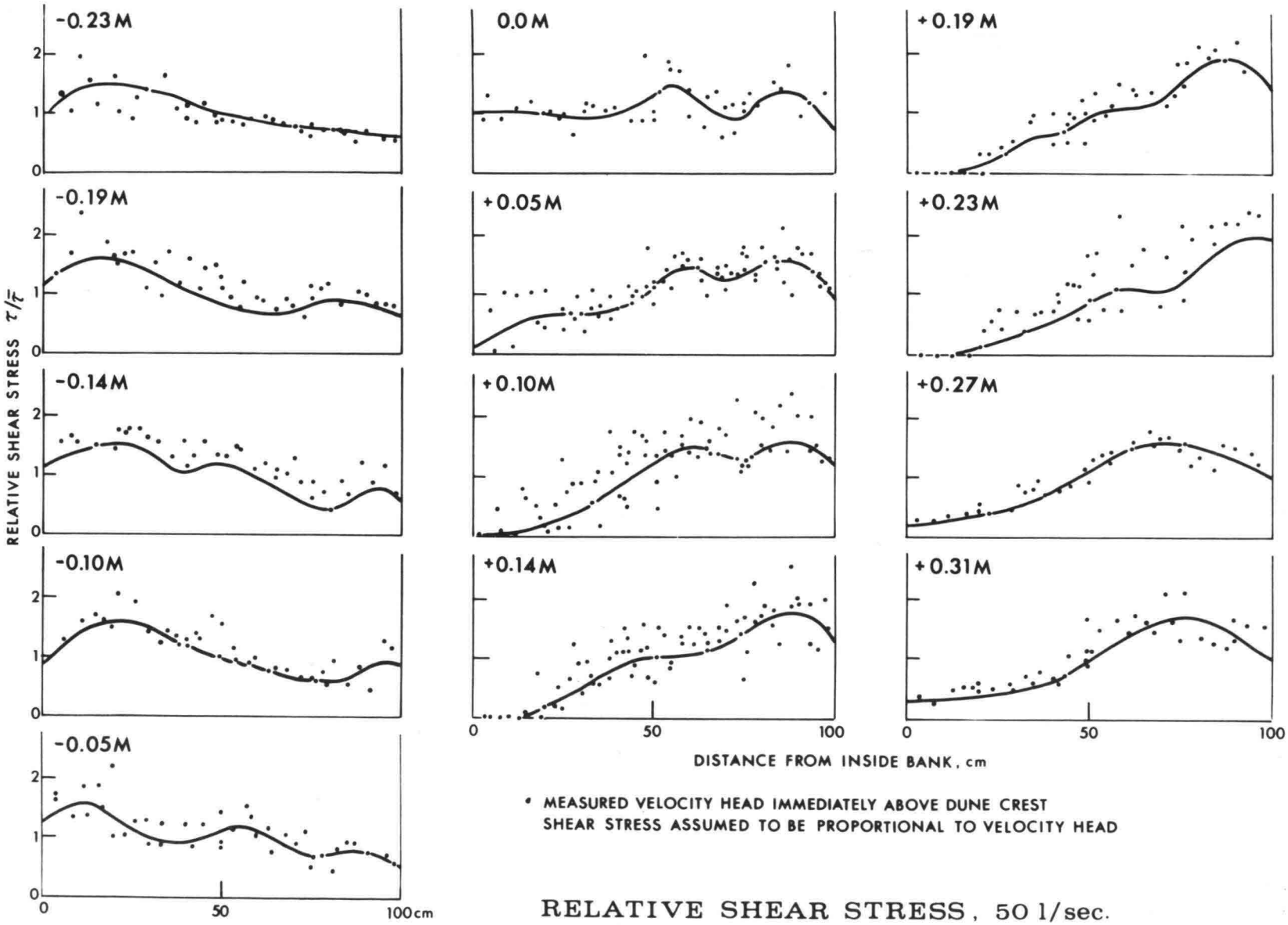
-0.23M
0.0M
+0.19M
-0.19M
+0.05M
+0.23M
-0.14M
+0.10M
+0.27M
-0.10M
+0.14M
+0.31M
-0.05M
RELATIVE SHEAR STRESS τ/τ̄
0
1
2
0
50
100
100cm
DISTANCE FROM INSIDE BANK, cm
* MEASURED VELOCITY HEAD IMMEDIATELY ABOVE DUNE CREST
SHEAR STRESS ASSUMED TO BE PROPORTIONAL TO VELOCITY HEAD
RELATIVE SHEAR STRESS, 50 l/sec.

Fig. 7C Run 50.

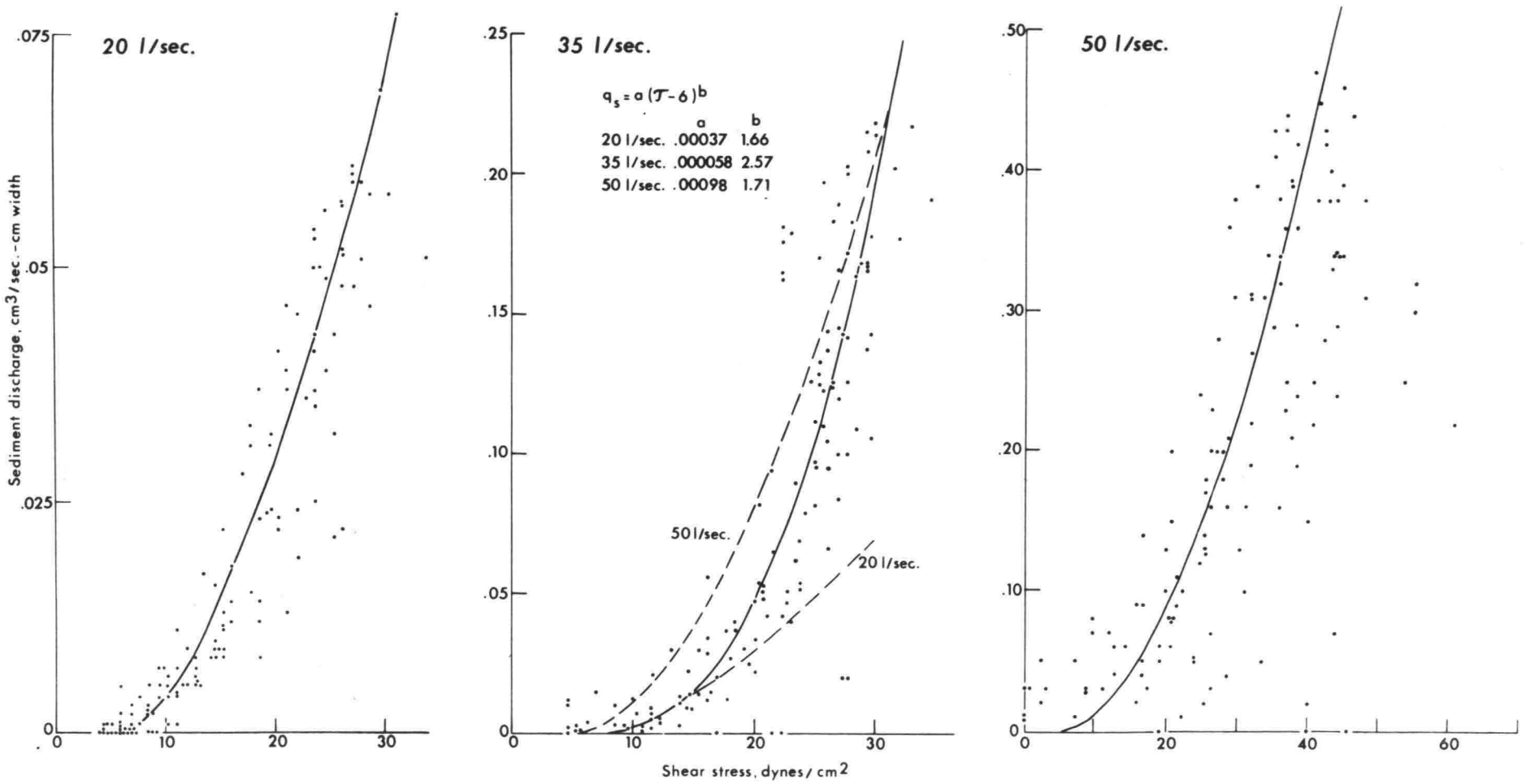

Fig. 8 Relation between local sediment discharge, q_s, and local shear stress, τ. Curves fitted by eye. Equations of curves shown in middle diagram.

where $\beta = \bar{\tau}/\bar{U}_{dc}^2$. The value of $\bar{\tau}$ is that given in Table 1, and $\bar{U}_{dc}$ is the velocity corresponding to the mean ΔP. This mean ΔP was determined from the areas under the curves in Fig. 7, not from the actual measurements. The values of β for Runs 20, 35, and 50 were 0.0245, 0.0219, and 0.0239 g/cm. The agreement is remarkable, considering the number of factors which contribute to β and which might be expected to change between runs, such as the mean height of the Preston Tube above the dune and the ratio of mean bed shear stress to maximum shear stress over the dune crests.

3.6 BANK SHEAR STRESS MEASUREMENTS

Shear stresses on the vertical channel banks were measured with the use of the 2 mm O.D. Preston Tube mentioned above. The static tube was separated from the total head tube and was fixed about 5 cm from the wall and 2 to 4 cm below the water surface. Measurements were made at depths of 1, 3, 5, 7... cm on both banks at the stations shown in Fig. 1. During Run 20, additional measurements were made on the concave bank midway between these stations from Sta -0.19M to Sta +0.23M. Repeated measurements at the same station and depth showed considerable variation due to migration of dunes on the bed, particularly in regions of higher shear stress and at higher discharges. To obtain reasonable average values, therefore, up to 8 measurements were made at each station and depth.

During Run 50 the Preston Tube was connected to the inclined manometer mentioned above. In Runs 10 and 35 the tube was connected to a differential pressure transducer and ΔP was recorded on a chart recorder. During Run 20 both methods were used. The chart record was calibrated at the beginning and end of each day's work, and occasionally more frequently, by applying a differential pressure equivalent to 6 mm of water head in steps of 1 mm. The calibration remained constant within about 2%. Readings at zero differential pressure were made frequently during the measurements.

3.7 "HELIX STRENGTH" MEASUREMENTS

The orientation of the velocity vector with respect to the channel centerline was determined near the water surface and near the bed with the use of a thread on the end of a needle. As before, a plastic dish set in contact with the water surface was used to facilitate observation. A protractor graduated in degrees was fixed on the dish. Measurements were recorded to the nearest degree or half degree. Accuracy varied from $\pm 1^\circ$ to $\pm 5^\circ$ depending on the intensity of macroturbulence. The angular difference between the orientation of the thread at the water surface and at the bed is considered to be a measure of the "strength" of the helical flow.

3.8 PREPARATION OF THE STABILIZED BED

For comparison with the movable-bed studies, shear-stress and helix-strength measurements were made in a 35 l/sec flow over a stabilized (cement) bed without dunes. The topography of the stabilized bed was determined from the bed elevation measurements at the end of Run 35. Cross-channel geometries at stations one half wavelength apart were averaged, so consecutive bends were mirror images of one another. The mean slope of the bed was reduced to 0.00075 to accommodate the reduction in friction factor due to elimination of the dunes. Measurements subsequently indicated that the slope should have been about 0.00092 to produce uniform flow with the depth and discharge used in Run 35. Due to undetected evaporation, the actual energy-gradeline slope during Run 35S was 0.00101. The difference between this slope and the bed slope is equivalent to a decrease in depth of about 2 mm or 2% through the test reach.

3.9 SHEAR-STRESS MEASUREMENTS ON THE STABILIZED BED

Shear stress measurements on the stabilized bed were made with the use of the 2 mm O.D. Preston Tube mentioned earlier, and with a 6 mm O.D. tube. All measurements were made with the use of the differential-pressure transducer and chart-recorder system already described. Initially measurements were made at ten evenly-spaced points in each cross section with the large tube, and at 9 intermediate points in each cross section with the small tube (Fig. 9).

For a given shear stress, the differential pressure recorded by the small tube is less than that recorded by the large tube because the former lies closer to the bed and hence "sees" a lower mean velocity. Thus ΔP measurements made with the use of the small tube were multiplied by 1.4 and plotted with the large-tube measurements (Fig. 9) before converting the ordinate to relative shear stress, $\tau/\bar{\tau}$. The factor 1.4 was obtained by evaluating Hwang and Laursen's (1963) equation (20) for the two different tube sizes. From measured velocity profiles it was estimated that $\frac{U_* k_s}{\nu}$ was between 7 and 20, so the constant D in the logarithmic velocity distribution equation,

$$\frac{U}{U_*} = \frac{1}{K} \ln \frac{y}{k_s} + D \qquad (7)$$

was taken as 9.6, and appropriate changes in the constants in Hwang and Laursen's equation were made. In this equation U is the velocity at a height y above the zero velocity datum, and other quantities are as defined previously.

Measurements made with the different tubes generally agreed very well (Fig. 9).

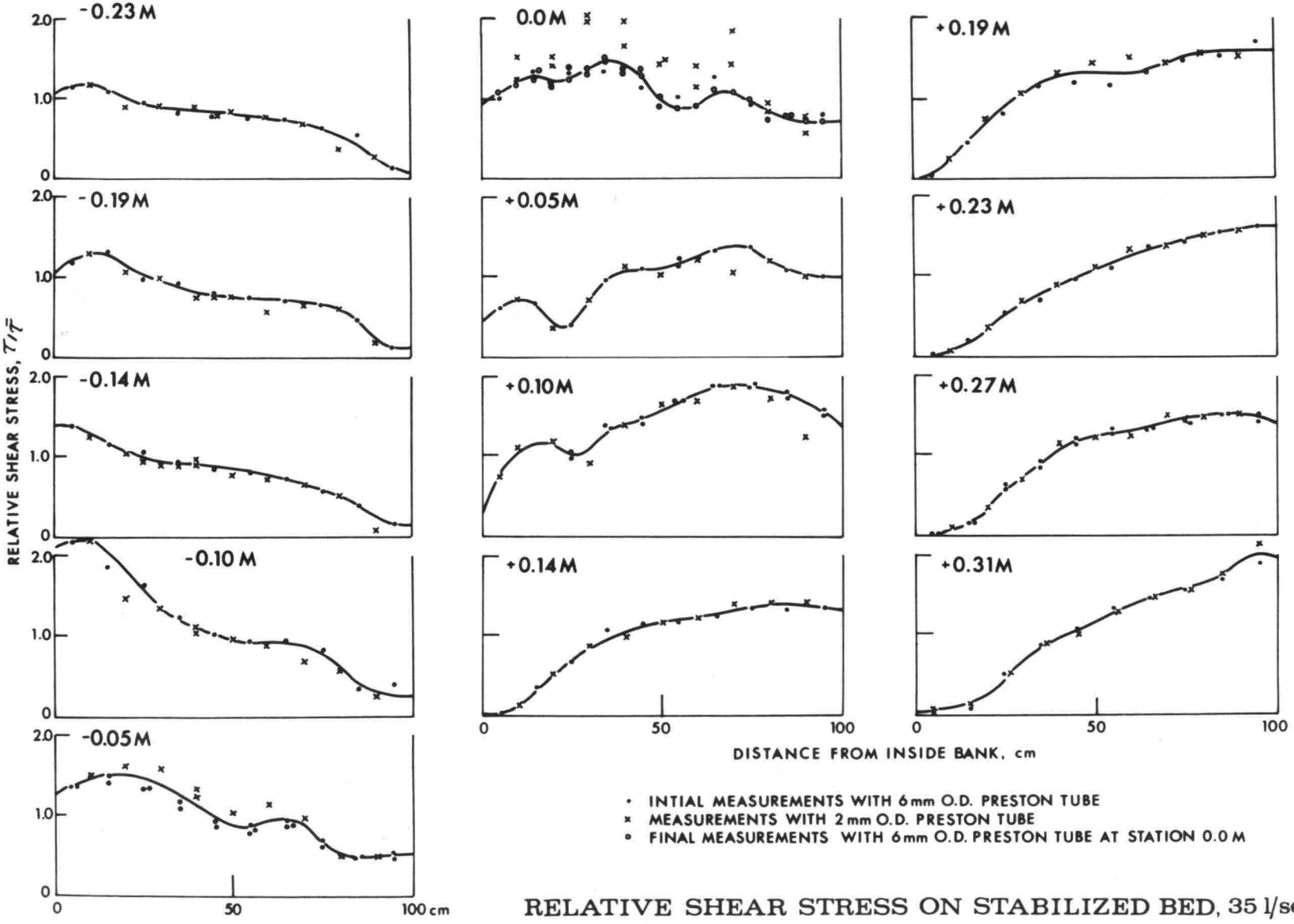

Fig. 9 Relative shear stress, $\tau/\bar{\tau}$, on stabilized bed.

Reproducibility was checked by periodically returning to points which had been measured sometime previously, and in most cases also proved to be excellent. Only at Station 0.0M was agreement particularly bad. To investigate this, a second set of 27 measurements was made at this station with the 6 mm tube. These proved to be somewhat more consistent and reproducible (Fig. 9).

4 RESULTS

Results of these various measurements are presented in Figs. 10 through 14. Bed elevation contours are shown in Fig. 10; in the lower two diagrams on Fig. 10B, the 0, +4, and -10 cm contours for each run are superimposed to facilitate comparison. An increase in discharge and depth results in an increase in the height and size of the point bar, an increase in depth of the deep on the outside of the bend, and perhaps a slight inward displacement of the 0 cm (or mean bed elevation) contour.

Contour maps in Fig. 11 show that "helix strength" increases markedly with discharge. Furthermore, the helix was stronger, further from the outside bank, and considerably broader in Run 35S (Fig. 11B) than in Run 35. This is probably because secondary currents were not damped as rapidly on the dune-free stabilized bed.

Sediment-distribution and shear-stress maps are presented in Figs. 12 and 13 respectively. These maps were prepared from the diagrams in Figs. 6, 7 and 9 by determining positions of the contours at each station and plotting these positions on a map of the channel. Where data from two cross sections one-half wavelength apart indicated two possible positions for a contour, both positions were plotted at both sections. Contours were sketched through the points and were smoothed to remove irregularities which were felt to be products of random error. Patterns were adjusted to satisfy the requirement of symmetry at sections M/2 apart.

The reliability of the maps can be estimated from the deviations of the smoothed contours from the plotted contour positions. The estimated standard error in the maps for Run 20 is $\pm$1/4 of a contour interval, for Runs 35 and 50, $\pm$1/2 of a contour interval, and for Run 35S, $\pm$1 contour interval. The lower reliability of the shear stress map for Run 35S is due to two factors:

1/ The curves in Fig. 9 were not adjusted to satisfy the sediment-discharge continuity condition, and

2/ It appeared that relatively small discrepancies between the geometry of the cement bed and that of the average sand bed resulted in substantial changes in shear stress. For example, the bed was probably about 1 cm too high at Sta +0.10M in Run 35S; this is apparently the reason for the high shear stresses measured here (Fig. 9).

With increasing discharge (or depth) the zone of high shear stress and high sediment discharge tends to move toward the convex bank and crosses the

M=13.2

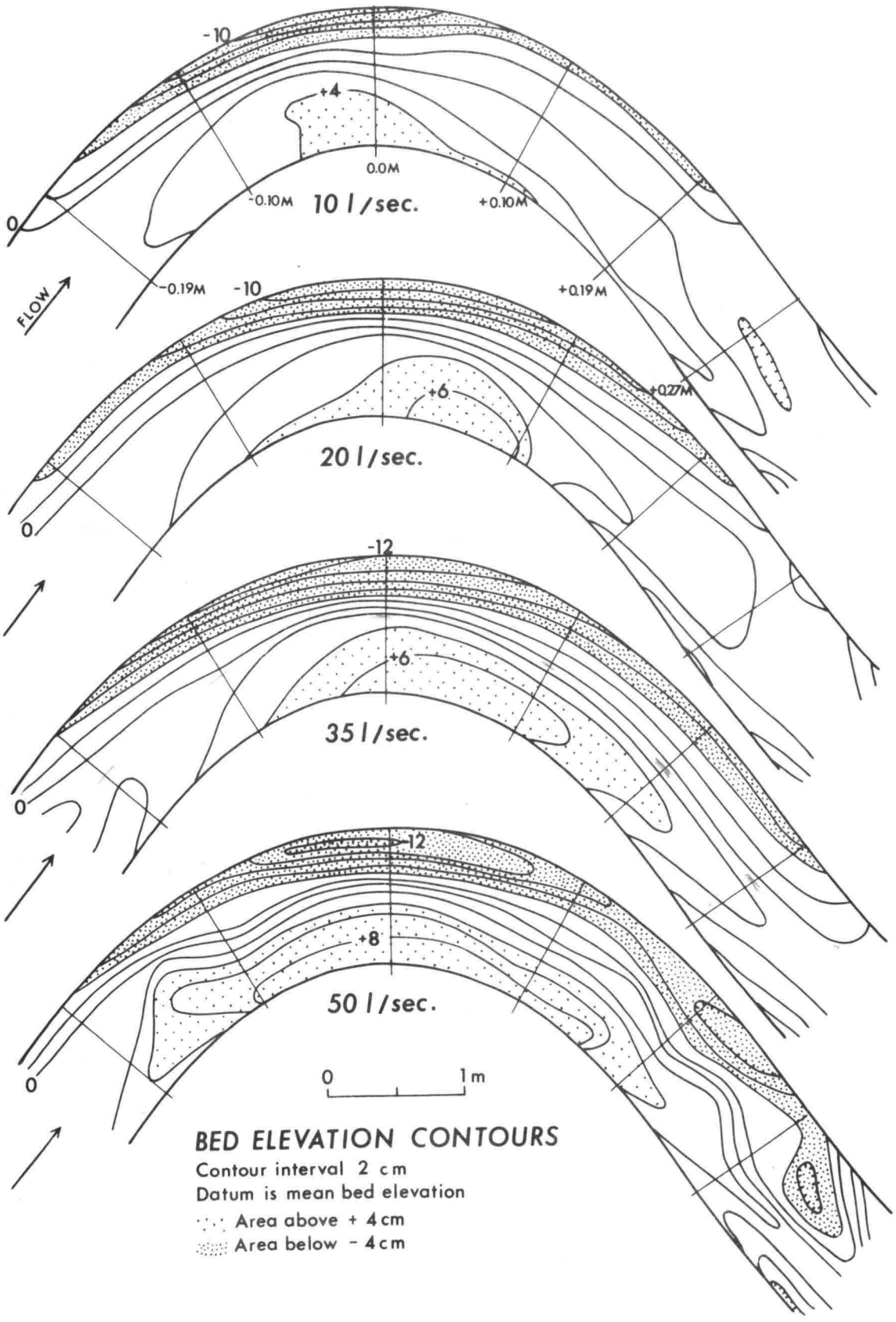

Fig. 10 Bed topography at different discharges. Depressions near Sta +0.27M in Run 50 are due to high, long-wave-length dunes which were not completely eliminated during smoothing. Slight differences between Runs 35 and 35S are due to smoothing and to fact that latter is based on average cross-channel geometries at stations M/2 apart. Fig. 10A

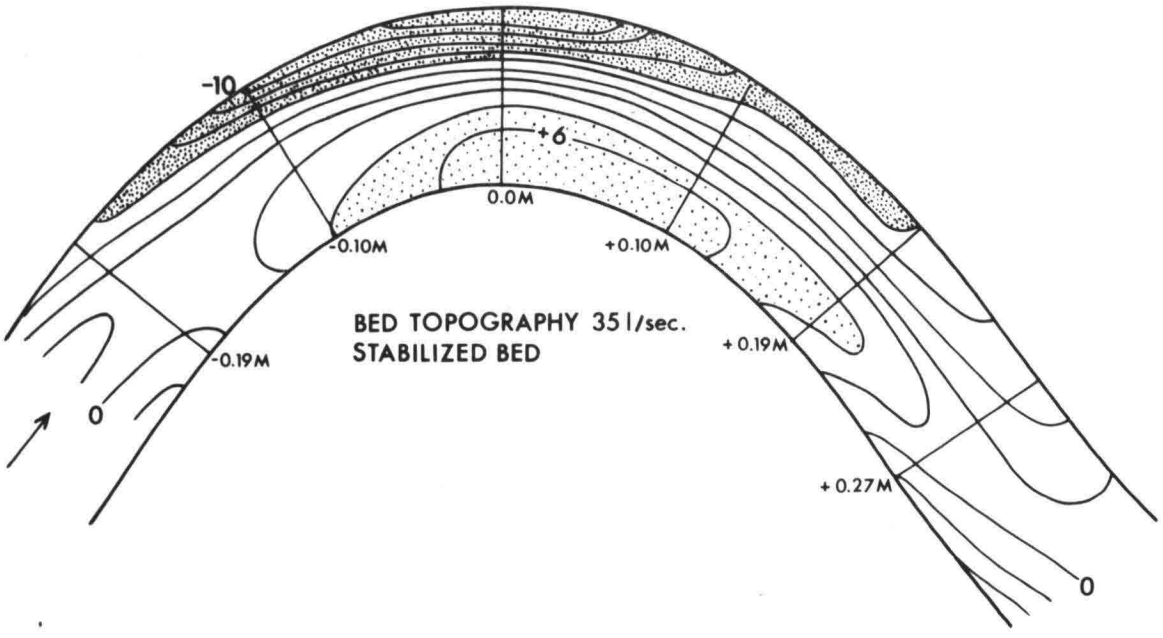

COMPARISON OF BED TOPOGRAPHIES DEVELOPED AT DIFFERENT DISCHARGES

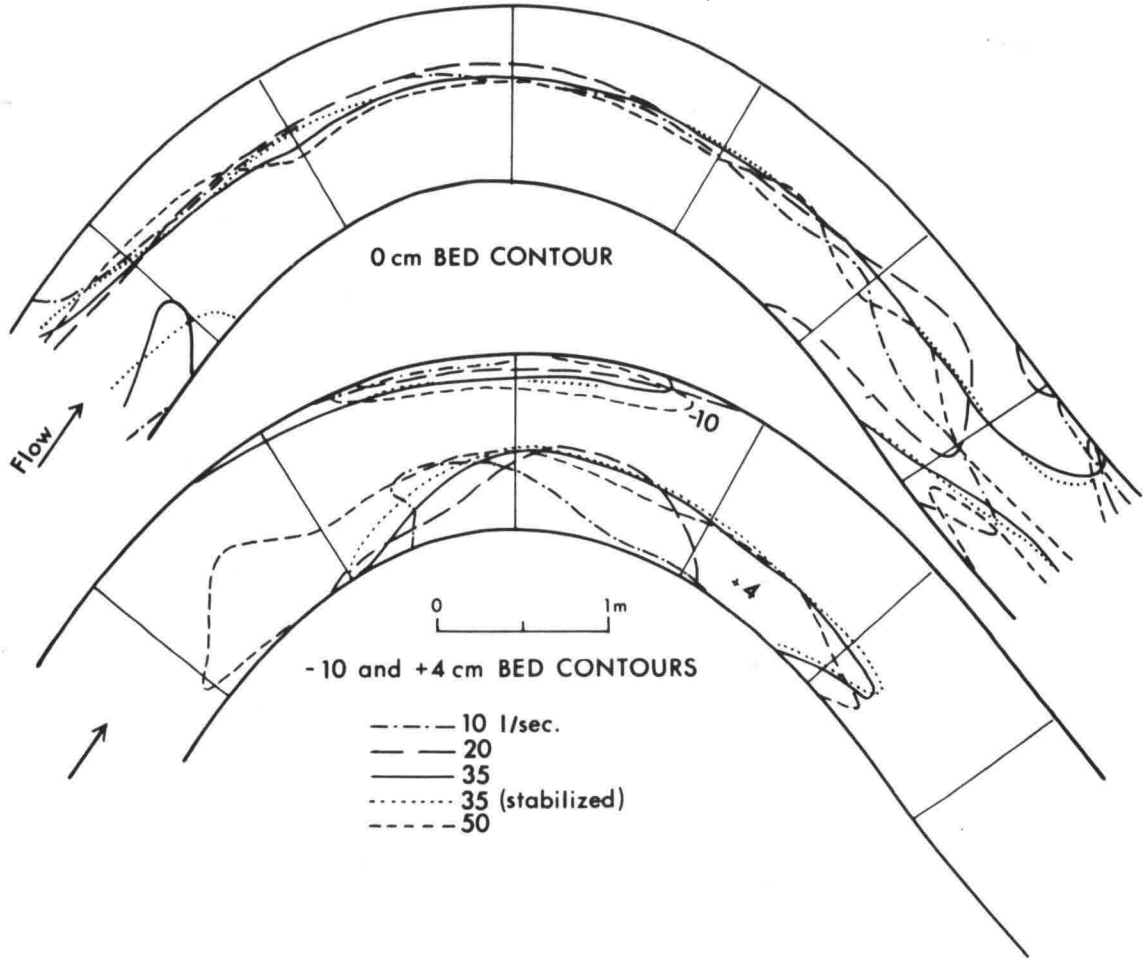

Fig. 10B

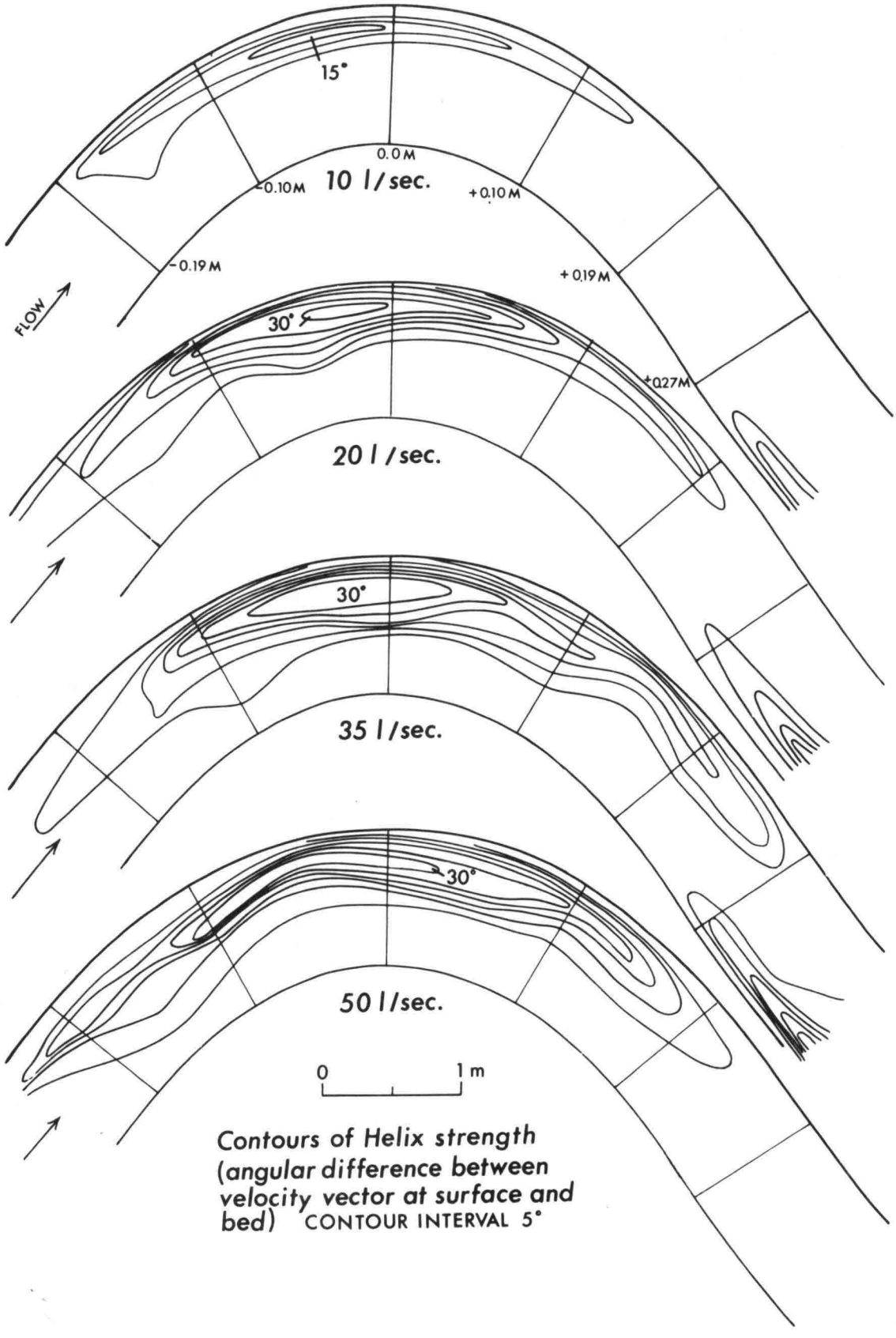

Fig. 11 Contours of "helix strength". Velocity vector at surface was outward toward outer bank, while that at bed was inward toward point bar. Measurements in Fig. 11A by Brian B. Dahlin. Fig. 11A

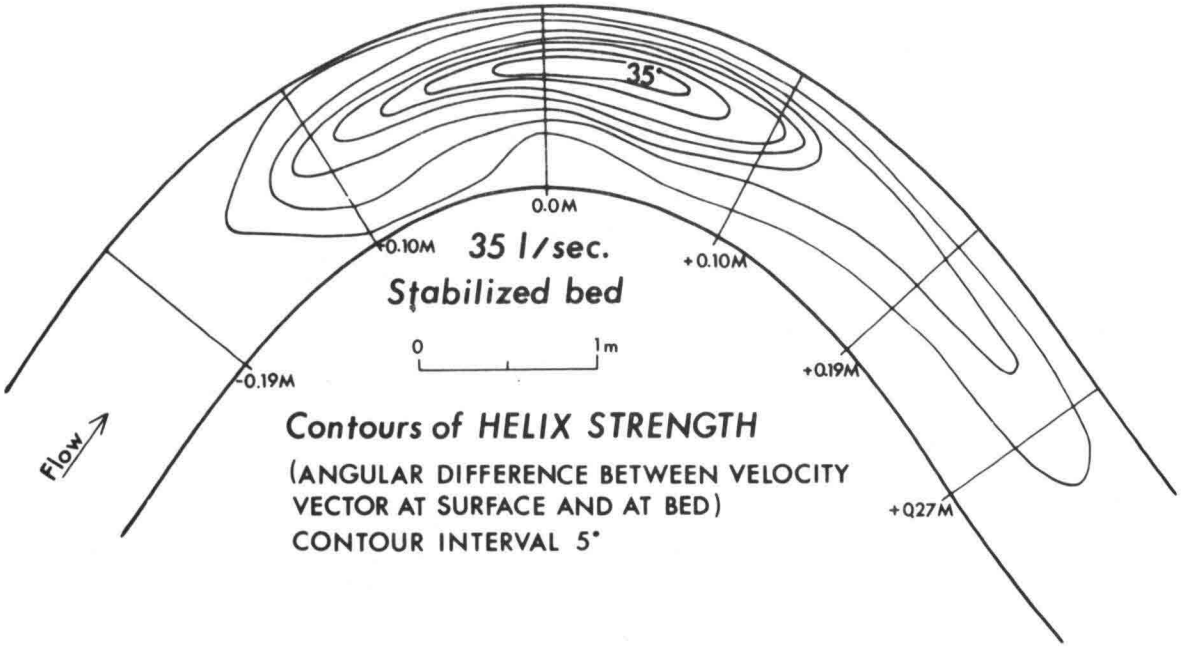

Fig. 11B

channel further downstream. This shift is presumably due to the increase in helix strength (Fig. 11). A similar inward shift of the zone of maximum shear stress apparently occurs with increasing discharge in natural rivers (Matthes, 1941), and may be responsible for the formation of chutes and chute cut offs (Matthes, 1951).

At higher discharges secondary maxima in both τ and q_s appear near the concave bank at about Sta-0.05M. These maxima are also thought to be a consequence of the helical flow, which brings higher velocity water down from the surface along the concave bank. Onishi et.al. (1972, p. 129) found a similar double maximum in the suspended sediment discharge. In their experiment the Froude number was 0.48 and W/d = 18. This suggests that the absence of such a pattern in Run 20 was due to the relatively low velocity (Froude number), not to the high width-depth ratio.

The shear stress distribution measured on the stabilized bed (Run 35S) is basically similar to that measured in Run 35 (Fig. 13). In Run 35S the maxima are closer to the convex bank, and the outer maximum is less prominent. The former difference is attributed to the greater strength of secondary flow in Run 35S (Fig. 11). The latter may be due to improper molding of the cement bed. At the end of Run 35S, several kilograms of sand were added at the inlet to see where deposition would occur. Longitudinal bars formed downstream from the point bars in each bend. These bars diverged from the up-valley bank, and at Sta 0.0M one coincided with the position of the outer maximum in τ. As noted earlier, (p. 5), such deposition is likely to cause an increase in shear stress. Thus had the cement bed been somewhat higher in this area, as apparently it should have been, the shear stress probably would have been higher also.

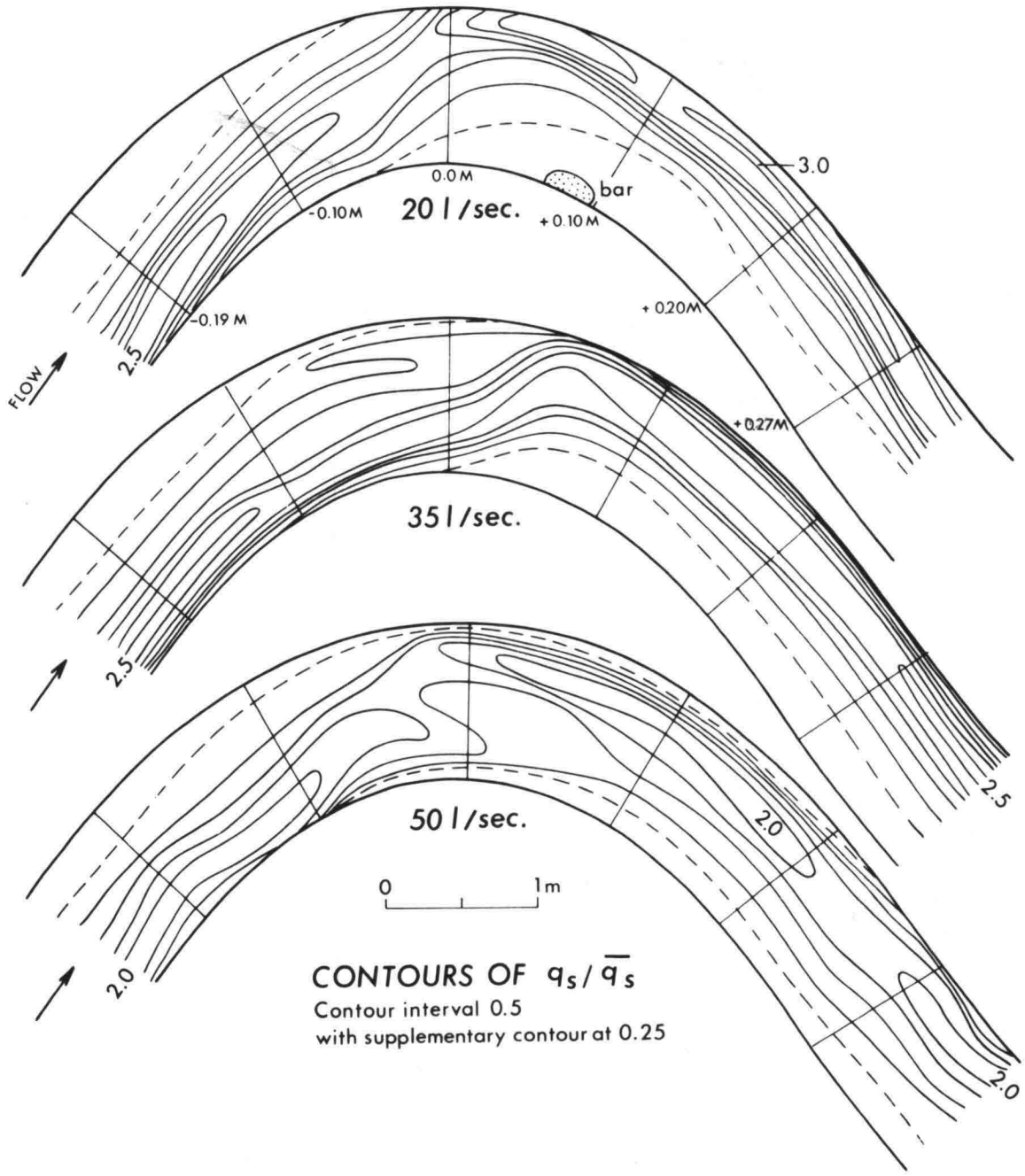

Fig. 12 Distribution of sediment discharge per unit width, q_s, at various discharges. Standard error approximately $\pm 1/4$ contour interval at 20 l/sec and $\pm 1/2$ contour interval at 35 and 50 l/sec.

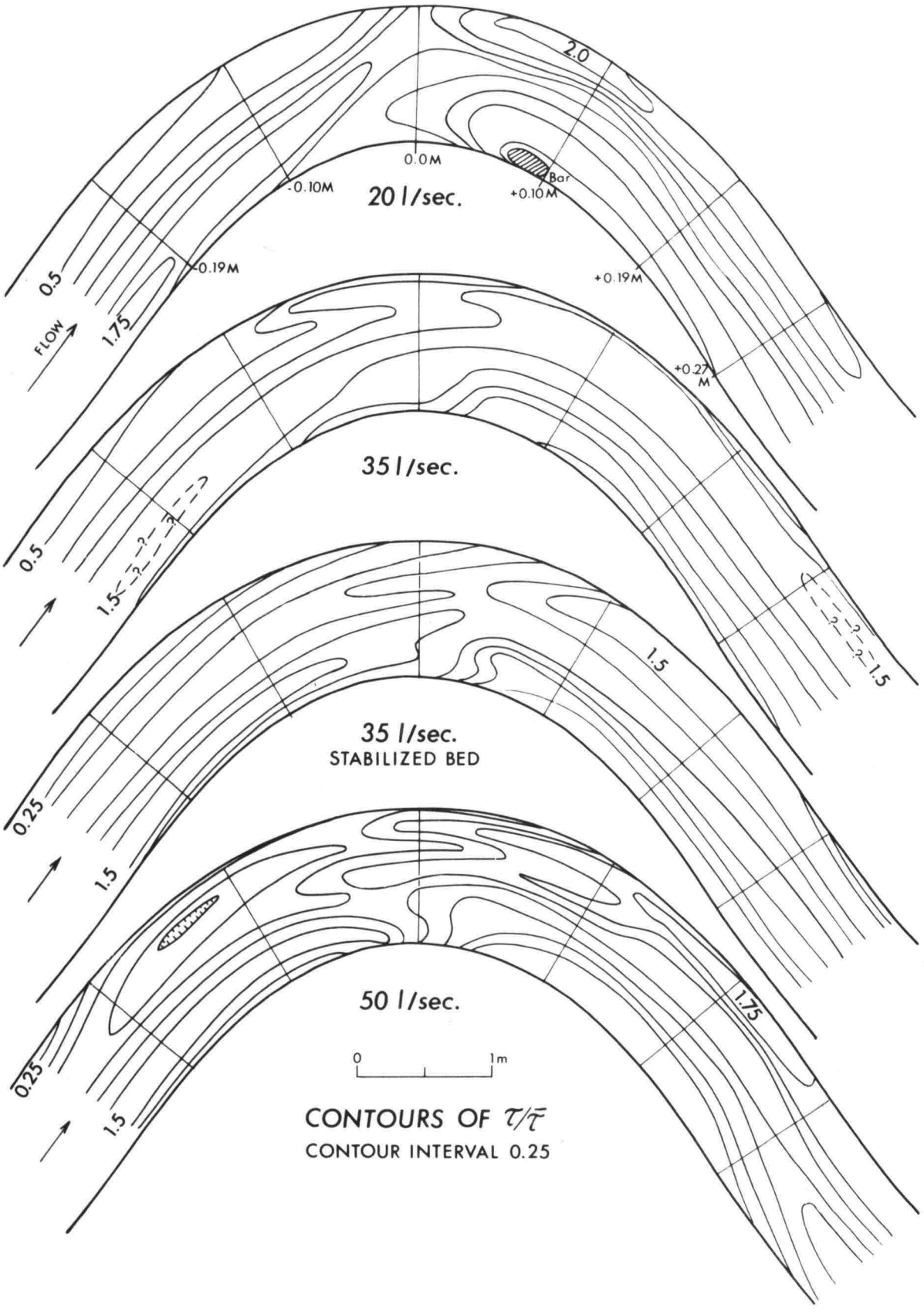

Fig. 13 Shear stress distribution at various discharges. Standard error approximately $\pm 1/4$ contour interval in Run 20, $\pm 1/2$ contour interval in Runs 35 and 50, and ± 1 contour interval in Run 35S.

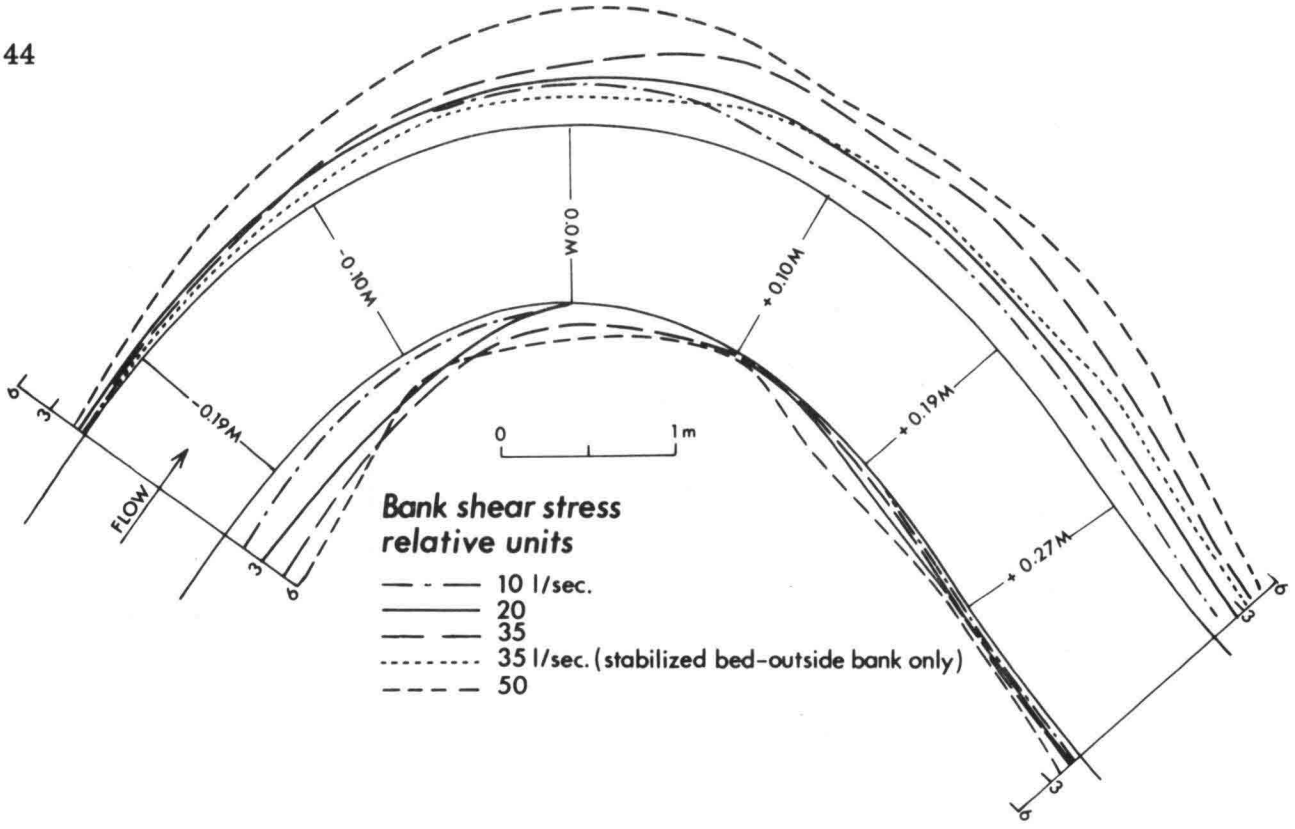

Fig. 14 Mean of bank shear stress measurements at depth of 1, 3, and 5 cm.

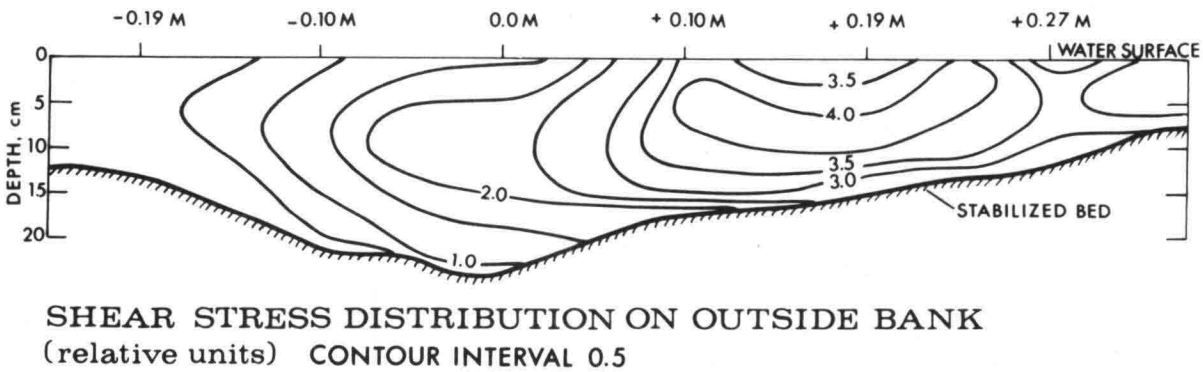

SHEAR STRESS DISTRIBUTION ON OUTSIDE BANK
(relative units) CONTOUR INTERVAL 0.5

Fig. 15 Relative shear stress distribution on outside bank during Run 35S.

Maps showing the distribution of bank shear stress are presented in Figs. 14 and 15. During the movable bed experiments, the maximum bank shear stress generally occurred within 5 cm of the water surface. Furthermore, shear stress measurements at greater depths were rather erratic due to passage of dunes on the bed. Therefore for these runs only the mean shear stress on the upper 5 cm of the bank is presented (Fig. 14). During Run 35S the maximum bank shear stress occurred at a greater depth, presumably due to the absence of dunes on the bed, and measurements were much more reproducible; the shear stress distribution over the entire bank is thus shown (Fig. 15).

In general shear stress on the outside bank increases to a maximum at about Sta +0.05M. It then declines slightly before rising to a second maximum near Sta +0.19M. This double maximum pattern occurred in all runs, and positions of the maxima did not appear to vary systematically with discharge. The upstream maximum occurs where high velocity water near the center of the channel upstream from the bend impinges against the concave bank downstream from the bend.

5 RELIABILITY OF BED SHEAR STRESS MEASUREMENTS

The reliability of the bed shear stress maps (Fig. 13) is affected by both random and systematic errors. In the movable bed runs the random error in any one measurement may be substantial. However by making many measurements at each cross section, by adjusting the curve through the measurements to satisfy the sediment-discharge continuity condition, by superimposing measurements from stations M/2 apart, and finally by smoothing the contours to eliminate local irregularities, the effect of these random errors on the final maps has been minimized. In the stabilized bed run the main sources of random error are probably differences between the stabilized bed geometry and the average or ideal geometry for a discharge of 35 l/sec. As in the movable-bed runs, these errors also have been minimized by superimposing measurements from stations M/2 apart and by smoothing contours to eliminate local irregularities.

Systematic errors are more difficult to identify and evaluate. Four possible sources of systematic error will be discussed. Firstly, in the movable bed measurements the height of the Preston Tube above dune crests may have varied. The tube was lowered to the point where scour of the crest was imminent. It is reasonable to suppose that the tube might have been systematically lower in zones of low shear stress. This, then, would have artificially accentuated the change in shear stress across the channel at stations in the straighter reaches (e.g. Stations +0.19M through +0.31M, Figs. 7). If, for example, the tube center was 1.5 mm above the crest near the inside bank and 3 mm near the outside bank, the relative shear stress, $\tau/\bar{\tau}$, would have been underestimated by 15 to 20 percent near the inside bank and overestimated by about 10 percent near the outside bank.

A second source of systematic error in the movable bed measurements is change in dune geometry with position in the channel. Because all measurements were made on dune crests, the shear stress estimated was the maximum for any given position. To the extent that the mean is a constant percentage of the maximum, this would not affect the maps. However over the point bar at Station 0.0M the bed was often nearly flat, and the mean and maximum may have been nearly equal. Such an error would have resulted in underestimating the shear stress on the inside of the bend and overestimating it on the outside. Thus the zone of high shear stress at Sta 0.0M may actually lie somewhat further downstream than shown. This could account for part of the difference between the maps for Runs 35 and 35S. The position of the secondary maximum near the outside bank at Sta 0.0M probably would not be affected, though its magnitude would be slightly.

A third source of systematic error in the movable-bed measurements is the decrease in the von Kármán constant, K, with increasing sediment concentration (Vanoni and Nomicos, 1959). Some rough calculations based on Fig. 11 of Vanoni and Nomicos' paper suggest that in the present experiments, $\tau/\bar{\tau}$ might be overestimated by 5 to 10 percent in regions of high shear stress and underestimated by a similar amount in regions of low shear stress. However comparison of the shear-stress distribution on the stabilized bed with that on the movable bed at the same discharge suggests that if anything the reverse is true. This argument is weak though, because we cannot say *a priori* that the shear stress distribution should be the same in stabilized-bed and movable-bed runs at the same discharge.

The final source of systematic error is variation in the von Kármán constant due to factors other than the concentration of suspended sediment. Rozovskii (1957), for example, showed theoretically that under certain conditions K may increase substantially through a bend. Unfortunately K is not easy to determine. Rewriting equation (7) in the form

$$U = \frac{U_*}{K} \ln \frac{y}{k_s} + U_* D \qquad (7')$$

we see that $\frac{U_*}{K}$ and $U_* D$ can be determined from a velocity profile measured near the bed if y and k_s are accurately known. (y is often not known precisely because the level at which U = 0 is some small distance, αk_s say, below the tops of roughness elements on the bed.) Then if D is known from, for example, graphs of D vs. boundary Reynolds number, U_* and K can be determined. Both α and k_s may vary slightly with position on the bed, and D may not be known accurately (see, for example, Meland and Norrman, 1966).

During the stabilized-bed experiments velocity profiles were measured at Stations -0.025M, +0.10M, and +0.27M. Measurements were made 35 cm from the concave bank. Each profile consisted of 10 velocity measurements, 7 of which were within 10 mm of the bed. All three profiles obeyed a logarithmic velocity destribution law within 9 mm of the bed. With k_s = 0.3 mm, D = 9.6, and α = 0.5, K was 0.79, 0.50, and 0.56 and U_*^2 was 6.0, 8.2, and 6.7 cm^2 per sec^2 at the three stations respectively. Increasing k_s to 0.5 mm or decreasing α to 0.3 resulted in an increase in K of 0.02 at all three stations, so K is fortunately not too sensitive to the exact values of α and k_s used. The observed variations in K bear no systematic relation to helix strength (Fig. 11B), orientation of the velocity vector at the bed, or longitudinal position in the channel.

Without additional measurements of K, further analysis of this effect is not possible. However variations in K in a longitudinal direction will have a relatively small effect on the contour patterns in Fig. 13 because contours have been smoothed, and because, in the movable bed runs, the shear-stress distribution at each section satisfies the sediment-discharge continuity condition. Cross-channel variations in K would have a more serious effect.

In conclusion, systematic errors probably contribute only slightly to the uncertainty in the contour maps in Fig. 13. The bulk of the uncertainty arises from random error. Until better measuring techniques are developed it will be difficult to reduce this error appreciably, and also difficult to evaluate more precisely the contribution of various sources of systematic error.

6 COMPARISON OF SHEAR-STRESS AND SEDIMENT-DISCHARGE DISTRIBUTIONS

It was suggested above that bed geometry is adjusted to provide, at each point on the bed, precisely the shear stress required to transport the sediment load supplied. The shear-stress and sediment-discharge maps (Figs. 12 and 13) support this hypothesis qualitatively. In an attempt to compare the measurements quantitatively, the quantity $G = (q_{s_{obs}} - q_{s_{calc}})/e$ was calculated at 10 points in each cross section. Contour maps of G are shown in Fig. 16. $q_{s_{calc}} = a(\tau - \tau_c)^b$ where a, b, and τ_c were determined from Fig. 8. $q_{s_{obs}}$ and τ were read from the curves in Figs. 6 and 7. e is the uncertainty in $(q_{s_{obs}} - q_{s_{calc}})$, and is calculated by assuming a standard error in measurement of 25% in τ and 33% in $q_{s_{obs}}$ over most of the channel. This uncertainty was increased to 100% at low values of τ and $q_{s_{obs}}$. These uncertainties are high because small uncertainties in the lateral positions of the curves in Figs. 6 and 7 may result in substantial errors in the estimated shear stress or sediment discharge at a particular point. Because a, b, and τ_c were not determined independently, the analysis is somewhat circular and the discussion which follows must be viewed accordingly.

If the standard errors in τ and q_s have been properly estimated, we expect that $|G| > 1$ over 1/3rd of the channel. That is, the actual error in τ and q_s should be less than the standard error approximately 2/3rds of the time. Furthermore the areas where $|G| > 1$ should be distributed more or less randomly over the channel.

In Runs 20 and 35 the areas of high $|G|$ are distributed more or less randomly over the channel, but the total area enclosed by the $|G| = 1$ contours is substantially less than a third of the bed area. Thus it would appear that the standard error was overestimated by perhaps factor of two for these runs. In Run 50, approximately a third of the bed area is enclosed by the $|G| = 1$ contours, and the areas are not randomly distributed. Such systematically high values of $|G|$ could reflect errors in τ, in q_s, or in the original hypothesis.

In the case of the large area of "expected deposition" in Run 50, q_s was probably overestimated. In Fig. 6C lines were generally drawn above the points representing dune-migration measurements because these measurements clearly underestimated q_s in the areas of higher sediment discharge; it was assumed, perhaps incorrectly, that this was also the case in areas of low sediment discharge. In contrast, the long zone of "expected erosion" on the outside of the bend is real. The cement bed of the flume was exposed frequently in this zone, so it represents an area where the bed geometry was not adjusted to provide as much sediment as

the flow could transport. This was primarily because the relatively strong secondary currents raking diagonally downward on the channel bank moved the sand away from the base of the bank. A similar area of "expected erosion" was present in Run 35. This zone obviously extends up the bank to the water surface as bank shear stresses are relatively high here (Fig. 14) and q_s is negligible.

In natural streams a similar zone of potential erosion exists along the outside bank downstream from the bend. Matthes (1941) and Parsons (1960), among others, have observed that this is where maximum bank erosion takes place, and it is this erosion that gives rise to an orderly down-valley migration of meanders (Matthes, 1941; Friedkin, 1945, Pl. 25). We thus conclude that although there appears to be a balance between τ and q_s over most of the bed, such a balance does not exist along the outside bank downstream from the top of the bend. In nature, of course, the problem is complicated by the fact that bank materials are generally more cohesive and resistant to erosion than bed materials. Furthermore, it is not clear that an increase in q_s will reduce the potential for erosion, or cause deposition, on the banks, as it does on the bed. On steep banks where material cannot be deposited, sediment in transport may in fact increase erosion through abrasion.

7 DISCUSSION

The results of this study suggest three modifications of current thinking on meanders. Firstly, the importance of secondary currents in determining bed geometry is often overstated. At higher velocities the helical flow appears to be responsible for a secondary maximum in the shear stress distribution near the outside bank upstream from the bend, and for an inward shift of the primary maximum in the bend. Downstream from the bend, secondary currents are also responsible for bringing sediment free water with high erosive potential to the bed (Fig. 16) (see also Onishi et.al. 1972, p. 142). However contrary to the conclusions of C. Yen (1970, p. 72) and Onishi et.al. (1972, p. 134) it is the sediment distribution, not secondary currents, which are primarily responsible for development of the point bar. Due to the momentum of the sediment and flowing water, and in spite of the secondary flow, most of the sediment in transport crosses the channel centerline in the bend (Fig. 13). Downstream from the bend this sediment is carried along the outside bank. The diffusion coefficient is apparently too low for appreciable lateral spreading of the sediment in the distance between bends. The sediment thus enters the next bend along its convex bank.

To provide the shear stress necessary to move this sediment, there is a gradual decrease in depth along the outside bank from the deep in one bend to the point bar in the next. This decrease in depth results in a continuous acceleration of the flow and hence in shear stresses which are consistently above average (Fig. 13). Downstream from the point bar along the inside bank there is a zone in which relatively little sediment movement occurs. Here depth increases downstream, and the consequent divergence of the flow results in shear stresses which are below average.

The conclusion that secondary currents are not responsible for the existance of the point bar is reinforced by Leopold and Wolman's (1960) observation that no single parcel of water completely crosses the channel in the bend. Thus we cannot say that secondary currents scour sediment from the deep on the outside of the bend and pile it up on the point bar on the inside. Friedkin (1945), in fact, observed that most sediment scoured from the outside of a bend ended up on the inside of the next bend downstream.

On the other hand anyone who has observed sediment movement in a laboratory meander will have seen sediment moving diagonally upward on the outer slope of the point bar. Thus while the existence of the point bar cannot be attributed to the secondary currents, the detailed geometry of the bar is at least partly controlled by them. For example, the stronger the secondary currents, the

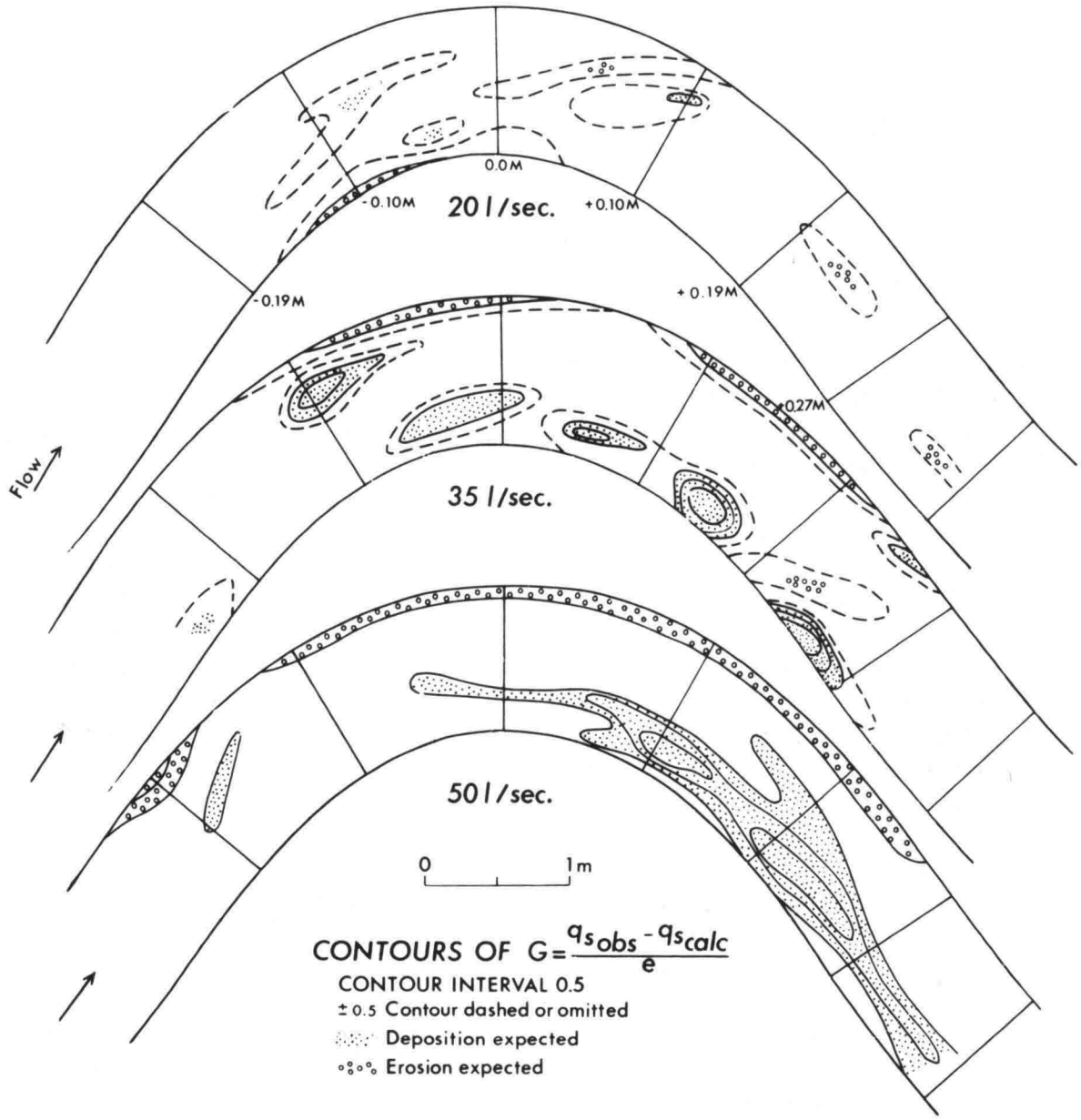

Fig. 16 Comparison of observed sediment discharge and sediment discharge calculated from shear stress distribution. Where G >1 deposition is "expected", and conversely.

steeper is the transverse slope of the outer part of the point bar (compare Figs. 10A and 11). The angle of repose of the bed material limits this effect at higher discharges.

The second modification of current thought concerns a redefinition of "the meander problem" in terms of system equilibrium. Suppose a gentle sand wave develops in the bed of an otherwise straight channel of uniform depth. If the straight, uniform-depth geometry of the channel represented a condition of stable equilibrium the sand wave would be eliminated and the channel would remain straight. However Engelund and Skovgaard (1973) have shown, by means of a stability analysis, that such an irregularity is likely to grow larger to form a bar. Furthermore, their analysis indicates that growth of one such bar on one side of a straight channel will promote growth of another bar a short distance downstream on the opposite side of the channel, and so on. This is in excellent agreement with the experimental observation of Ackers and Charlton (1970), among others, that alternating bars develop more or less simultaneously along the channel, and that such bars precede meander formation. As the bars increase in height, they deflect the flow against the opposite banks, which eventually begin to erode to form bends.

Thus theoretical analysis, model studies, and the commonly-observed geometry of natural streams all suggest that for a large variety of flow conditions found in nature, straight channels represent, at best, a condition of unstable equilibrium, such that a departure from this equilibrium condition sets up forces which cause the system to change still further away from the straight condition. Eventually the system achieves a new geometry with a series of bends. The wavelength of these bends is about 10 times the channel width and 4 to 5 times the radius of curvature (Leopold and Wolman, 1960).

This new geometry is dynamic because erosion continues along the down-valley bank and deposition on the up-valley bank. If the rate of erosion parallel to the valley axis is equal at all points on the down-valley bank, the meanders will migrate uniformly down valley without changing shape (Fig. 17). If, in addition, small departures from this shape result in forces, presumably shear stresses on the bank, which tend to reestablish it, the system is, by definition, in stable equilibrium. Such departures should be expected to occur frequently and more-or-less at random in nature due to local inhomogeneities in bank materials, vegetation, and so forth (Langbein and Leopold, 1966, p. 45; Matthes, 1941, p. 635; Friedkin, 1945, pp. 15-16). Thus natural meander trains should not be expected to be perfectly symmetrical, but if a stable equilibrium geometry exists, they will constantly tend toward this ideal.

The "meander problem" can thus be rephrased as follows: Under a large variety of flow conditions found in nature, straight channels are apparently unstable. Is the commonly-observed meander geometry a stable geometry, and if so why?

Some published observations bear on this problem. Firstly, measurements made during the present study suggest that, as a first approximation, changes in discharge change only the magnitude, and not the distribution of mean bank shear stress (Fig. 14). This is consistent with Schumm's (1967) finding that a meander

of a given geometry can carry a higher discharge if the banks are composed of more cohesive materials.

Secondly, Onishi et.al. (1972) conducted movable-bed experiments in a channel with a wavelength width ratio of 13, and in a channel with the same wavelength but only half as wide. Thus in the latter the wavelength/width ratio was double or triple that commonly found in nature. They found that the velocity distribution across the channel was much more uniform in the narrower channel. Thus shear stresses on the up-valley bank would be higher in the narrower channel. This is consistent with Bagnold's (1960) observation that the ratio $\underline{R/W}$ apparently determines when separation will occur along the convex bank downstream from a bend. $\underline{R}$ is the radius of curvature of the centerline of the bend. Separation generally occurs when $\underline{R/W}$ is between 2 and 3. This is true both in open channels and in pipes, and thus reflects some fundamental property of flow in a bend. In the present channel $\underline{R/W}$ was about 2.4, and separation occurred or was incipient in all runs. As a result, shear stresses were very low on the up valley bank (Fig. 14).

By combining results of the present study with the observations of Bagnold (1960), Schumm (1967), and Onishi et.al. (1972), we can offer a partial explanation for the apparent stability of the commonly observed meander geometry. We consider $\underline{Q}$, $\underline{Q_s}$, and sediment characteristics to be independent variables, and assume the river slope is adjusted to carry $\underline{Q_s}$ with the available $\underline{Q}$. We further assume that width is determined by $\underline{Q}$ and by the cohesiveness of the bank materials (Schumm, 1960). Thus once the river starts to meander, we need not be concerned by possible changes in $\underline{W}$. Finally we will discuss only the bank labeled A-A'-A" in Figure 17, and assume that the width remains constant through appropriate adjustments of the other bank.

For uniform down-valley migration of a meander, bank erosion must be zero at points A, A' and A" (Fig. 17). Furthermore the amount of erosion at any point between A and A' must equal the amount of deposition at the corresponding point between A' and A". We assume that erosion is occurring continuously and that it is necessary only to balance this erosion with an equal amount of deposition between A' and A". It is reasonable to assume that deposition will occur when $\underline{R/W}$ has a value close to that at which separation occurs. If $\underline{R}$ is too large, Onishi et.al. (1972) experiments suggest that τ will be too high for deposition between A' and A" so the bank A-A' will move down valley faster than bank A'-A", thus decreasing $\underline{R}$ and $\underline{R/W}$ until separation is imminent or actually occurs. Conversely, if $\underline{R}$ is too small, a wide zone of separated flow will occur and deposition on bank A'-A" will exceed erosion on bank A-A', thus increasing $\underline{R}$ and $\underline{R/W}$.

With R and W thus specified, we need to know the angle ω and the length, S, of the straight reach[1] (Fig. 17) to completely determine meander geometry. It is intui-

---

[1] It will be noted that four variables are required here, whereas in the sine-generated geometry (eqn 1) there are only three ($\underline{W}$, ω, and $\underline{M}$). The sine-generated geometry is thus more restrictive. Empirically it provides a good approximation to the geometry of natural meanders because $S \rightarrow 0$ in nature.

tively reasonable to expect that varying ω and S will vary the distribution of shear stress on the down-valley bank and hence the pattern of erosion there. We may thus ask whether some particular combination of ω and S will lead to the pattern of erosion sketched in Figure 17, and why. Measurements of bank shear stress on movable-bed fixed-bank channels with a variety of geometries would probably answer the first part of this question. The pattern of bank shear stress is probably controlled by secondary currents and bed geometry. Thus to answer the second part of the question these should be determined also.

There remains, of course, the possibility that there is no combination of ω and S which will result in uniform down-valley migration of meanders. For example, the pattern of bank erosion might be such that ω and S increase continually until a cutoff occurs and the channel returns, at least locally, to a straight geometry. Such a cyclic pattern is not, however, consistent with the laboratory observations of Friedkin (1945) and Ackers and Charlton (1970). These observations suggest that a stable geometry, in which meanders migrate continuously down valley, is indeed attained. Nor is a cyclic change in geometry consistent with the seemingly well-defined correlation between wavelength and width in natural meanders. Caution should be exercised here, however, because ω and S could vary with time in such a way that λ/W remained nearly constant over a substantial percentage of the time required for the cycle.

The third modification of current thought concerns the argument that meandering is the "most probable" geometry for a river (Langbein and Leopold, 1966; Yang, 1971). The analogy with statistical thermodynamics which is used in this argument is incomplete because the random variable has not been identified. In statistical thermodynamics one random variable is the movement of a molecule. Because there are such a vast number of molecules of air in a room, for example, we cannot know where every molecule is as a function of time. However because there are so many molecules, and because they interact so frequently, we can represent certain gross characteristics of the system by means of the ideal gas law. On the other hand, if the walls of our room were composed of a patchwork of materials. all of which were very flexible and elastic, we could not determine the shape of the room unless we knew the elastic constants of each of the materials and the location of that material in the wall. Furthermore if we heated one part of the room and cooled another part, the shape of the room would depend not only on the behavior of the air as described by the ideal gas law, but also on the rate at which energy was put into the system by the heater and removed by the cooler, and on the relative positions of the heater and cooler in the room. Similarly, certain characteristics of the behavior of water in an open channel can be described statistically. An excellent example is the suspended load distribution equation (Vanoni and others, 1963) which is based on the interaction between a large number of turbulent eddies and a large number of grains of sediment in suspension. However the distribution of turbulence and velocity in the flow, and the distribution of shear-stress on the banks are not random. Perturbations of the bed may well be stochastic, but the growth of some perturbations to form alternate bars is not (Engelund and Skovgaard, 1973); if it were, the bars would not have a well defined spacing along the channel. As suggested above that the irregularity of meander trains may be treated stochastically, as it could result from random variations in the erodibility of

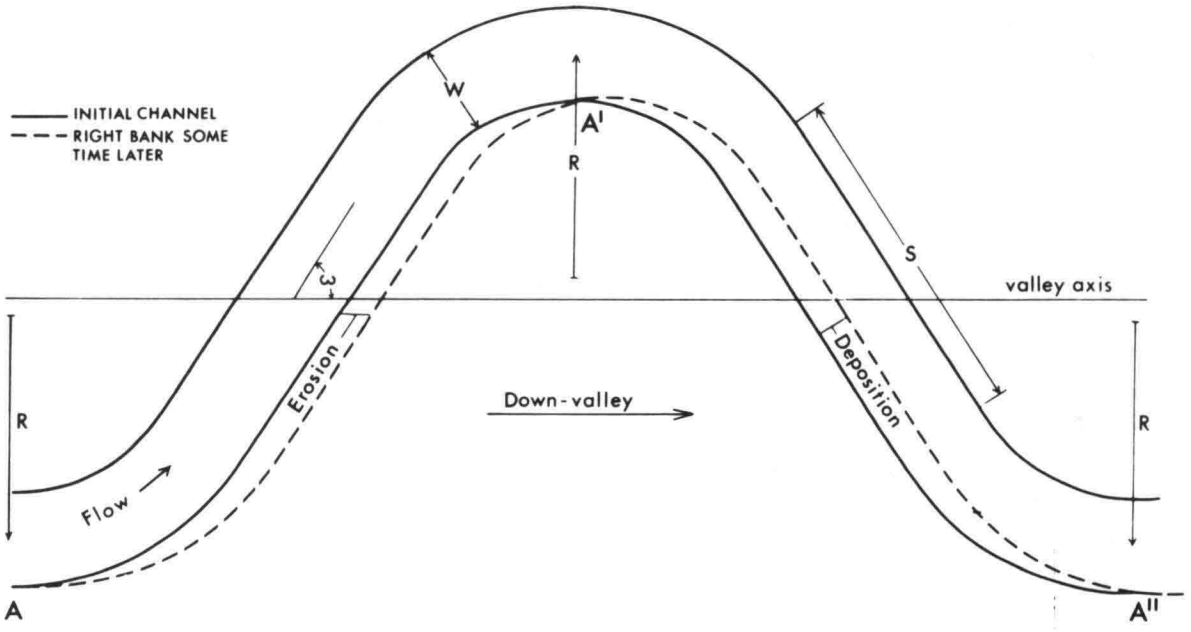

Fig. 17 Requirements for uniform down-valley migration of meander bends.

Floodplain materials encountered by the down-valley migrating bends. However to try to explain the shape of the average bend, or even the tendency toward bend development, by application of the laws of statistical thermodynamics would appear to be as fruitless as trying to determine the shape of our elastic room by applying only the ideal gas law. Until the random variable is properly identified and discussed, such attempts, although philosophically intriguing, must be viewed with considerable skepticism.

8 REFERENCES CITED

Ackers, P., and Charlton, F.G., 1970: The geometry of small meandering streams. Inst. of Civ. Eng. Proc. Suppl. XII, Pap. 732BS, p. 289-317.

Bagnold, R.A., 1960: Some aspects of the shape of river meanders. U.S. Geol. Surv. Prof. Pap. 282-E, p. 135-144.

Brooks, N.H., 1958: Mechanics of streams with movable beds of fine sand. Trans. Amer. Soc. Civ. Eng. Vol. 123, p. 526-549.

Creager, J.S., Smith, J.D., and Sternberg, R.W., 1969: Investigations of turbulent boundary layers and sediment transport phenomena as related to shallow marine environments. Part III; studies of non-uniform boundary layer flows. University of Washington, Dep. of Oceanogr. Rep. RLO-1752-13, 121 p.

Engelund, F., and Skovgaard, O., 1973: On the origin of meandering and braiding in alluvial streams. J. Fluid Mechanics. Vol. 57, Part 4, p. 289-302.

Friedkin, J.F., 1945: A laboratory study of the meandering of alluvial rivers. U.S. Waterways Exp. St., Vicksburg, Miss., 40 p.

Hwang, L.S., and Laursen, E.M., 1963: Shear measurement technique for rough surfaces. J. Hydr. Div., Amer. Soc. Civ. Eng., Vol. 89, No. HY2, p. 19-37.

Ippen, A.T., and Drinker, P.A., 1962: Boundary shear stresses in curved trapezoidal channels. J. Hydr. Div., Amer. Soc. Civ. Eng., Vol. 88, No. HY5, p. 143-179.

Langbein, W.B., and Leopold, L.B., 1966: River meanders - Theory of minimum variance. U.S. Geol. Surv. Prof. Pap. 422-H, p. H1-H15.

Leopold, L.B., and Maddock, T., Jr., 1953: The hydraulic geometry of stream channels and some physiographic implications. U.S. Geol. Surv. Prof. Pap. 252, 57 p.

Leopold, L.B., and Wolman, M.G., 1957: River channel patterns: braided, meandering, and straight. U.S. Geol. Surv. Prof. Pap. 282-B, p. 39-85.

———— 1960: River Meanders. Geol. Soc. Amer. Bull., Vol. 71, p. 769-794.

Leopold, L.B., Wolman, M.G., and Miller, J.P., 1964: Fluvial processes in geomorphology. Freeman & Co., San Francisco, 522 p.

Mackin, J.H., 1948: Concept of a graded river. Geol. Soc. Amer. Bull., Vol. 59, p. 463-512.

Matthes, G.H., 1941: Basic aspects of stream meanders. Trans. Amer. Geophys. Union, p. 632-635.

———— 1951: Paradoxes of the Mississippi. Sci. Am., April.

Meland, N., and Norrman, J.O., 1966: Transport velocities of single particles in bed-load motion. Geogr. Ann., Vol. 48, Ser. A, p. 165-182.

Onishi, Y., Jain, S.C., and Kennedy, J.F., 1972: Effects of meandering on sediment discharges and friction factors of alluvial streams. Iowa Inst. of Hydr. Res. Rep. No. 141, University of Iowa, Iowa City, Iowa, 150 p.

Parsons, D.A., 1960: Effects of flood flow on channel boundaries. J. Hydr. Div., Amer. Soc. Civ. Eng., Vol. 86, No. HY4, p. 21-34.

Rouse, H., 1950: Engineering Hydraulics. Proceedings 4th Hydraulics Conference, Iowa Inst. of Hydr. Res., John Viley & Sons, New York, 1039 p.

Rozovskii, I.L., 1957: Dvizhenie vody na povorote otkrytogo rusla: Institut Gidrologii i Gidrotekhniki Akad. Nauk. UKr. SSR. Kiev. English Translation (title: Flow of water in bends of open channels) by Y. Prushansky. PST Cat. No. 363, Jerusalem, 1961, 233 p.

Schumm, S.S., 1960: The shape of alluvial channels in relation to sediment type. U.S. Geol. Surv. Prof. Pap. 352-B, p. 17-30.

———— 1967: Meander wavelength of alluvial rivers. Science, Vol. 157, p. 1549-1550.

Simons, D.B., Richardson, E.V., and Nordin, C.F., Jr., 1965: Bedload equation for ripples and dunes. U.S. Geol. Surv. Prof. Pap. 462-H, p. H1-H9.

Suga, K., 1967: The stable profiles of the curved open channel beds. Proc. 12th Conference, Int. Assoc. Hydr. Res. Sept. 11-14, Colorado State University at Fort Collins, p. 487-495.

Vanoni, V.A., and Brooks, N.H., 1957: Laboratory studies of the roughness and suspended load of alluvial streams. Calif. Inst. Tech. Sed. Lab. M.R.D. Ser. Rep. No. 11, 121 p.

Vanoni, V.S., and Nomicos, G.N., 1959: Resistance properties of sediment-laden streams. J. Hydr. Div., Amer. Soc. Civ. Eng., Vol. 85, No. HY5, p. 77-107.

Vanoni, V.A., and others, 1963: Sediment transportation mechanics: Suspension of Sediment. J. Hydr. Div. Amer. Soc. Civ. Eng., Vol. 89, No. HY5, p. 45-76, (by the Task Committe on Preparation of sedimentation manual, Committee on Sedimentation, ASCE Hydraulics Division, P.C. Benedict, D.C. Bondurant, J.E. McKee, C.R. Miller, J. Smallshaw, and V.A. Vanoni, Chairman).

Yang, C.T., 1971: On river meanders. J. Hydr., Vol. 13, p. 231-253.

Yen, B.C., 1965: Characteristics of subcritical flow in a meandering channel. Iowa Inst. Hydr. Res. Publ., 76 p.

Yen, C.L., 1970: Bed topography effect on flow in a meander. J. Hydr. Div., Amer. Soc. Civ. Eng., Vol. 96, No. HY1, p. 57-74.

Nr 15 Håkanson, L., 1972: Sambandet mellan kvicksilverförekomst och sedimentologisk miljö i Ekoln. Del 3. Transport och deposition av kvicksilver.
The Relation between Mercury Distribution and Sedimentological Environment in Lake Ekoln. Part 3. Transportation and Deposition of Mercury.

Nr 16 Nilsson, B., 1972: Sedimenttransport i svenska vattendrag. Ett IHD-projekt. Del 2. Avrinningsområden, stationer och resultat 1967-69.
Sediment Transport in Swedish Rivers. An IHD-Project. Part 2. Catchment Areas, Stations and Results in 1967-69.

Nr 17 Hjorth, S., 1972: Torne och Kalix älvar. Del 2. Materialtransport 1967-69.
The Torne and Kalix Rivers. Part 2. Suspended and Dissolved Load in 1967-69.

Nr 18 Larsson, R.Å. & Sundborg, Å., 1972: A Photogrammetric Instrument System in Geo- and Bioscientific Research and Teaching.
Ett fotogrammetriskt instrumentsystem för geovetenskaplig och biologisk forskning och undervisning.

Nr 19 Nilsson, G. & Martvall, S., 1972: Öreälven och dess meanderlopp. En fluvialmorfologisk studie.
The Öre river and its meanders. A study of fluvial morphology.

Nr 20 Martvall, S. & Nilsson, G., 1972: Experimental Studies of Meandering. The transport and deposition of material in curved channels.

Nr 21 Lindell, T. & Kvarnäs, H., 1973: A Study of the Interaction between Lake Water and River Water.

Nr 22 Strömquist, L., 1973: Geomorfologiska studier av blockhav och blockfält i norra Skandinavien. Geomorphological studies of blockfields in northern Scandinavia.

Nr 23 Nilsson, J., 1973: An attempt to compute channel flows.

Nr 24 Aronsson, G., 1973: A new method for calculating the recession of slopes.

Nr 25 Axelsson, B. & Håkanson, L., 1973: Kvicksilver i södra Vätterns, Ekolns och Björkens sediment. Mercury in the Sediments of Southern Lake Vättern, Lake Ekoln, and Lake Björken.

Nr 26 Lindström, E, 1974: Deglaciation, sediment och högsta kustlinje i nordvästra Ångermanland.
Deglaciation, Sedimentary Deposits, and the Highest Late Glacial Shore Line in N.W. Ångermanland, Sweden.

Nr 27 Sundborg, Å., 1973: Indalsälven, Ljungan, Ljusnan, Dalälven, Klarälven. Geovetenskapliga naturvärden.

Nr 28 Denis, R., 1974: Late Quaternary Geology and Geomorphology in the Lake Maskinongé area, Quebec.

Nr 29 Ehlert, K. et.al., 1974: Effekter på vattenkvalitén i bäckar vid skogsgödsling med ammoniumnitrat och urea.

Nr 30 Hooke, Roger LeB, 1974: Shear-stress and sediment distribution in a meander bend.